INDOLE DERIVATIVES AS CORE STRUCTURAL MOTIFS IN MOLECULAR ORGANIC PHOTOACTUATORS

DOI: http://dx.medra.org/10.17374/targets.2022.25.381

Nadja A. Simeth,[a] Stefano Crespi[b]

[a]*Institute of Organic and Biomolecular Chemistry, Georg-August University of Göttingen, Tammannstraße 2, 37077 Göttingen, Germany*

[b]*Stratingh Institute for Chemistry, University of Groningen, Nijenborgh 4, 9747AG Groningen, The Netherlands*

(e-mail: nadja.simeth@uni-goettingen.de, s.crespi@rug.nl)

Abstract. *Indole and its derivatives are extremely versatile structures that impact an extraordinary broad range of disciplines in the chemical sciences. They represent a useful platform in organic synthesis which allows diverse functionalizations and are key scaffolds in both medicinal chemistry and the dye industry. Indeed, introducing an indole derivative in a molecule influences its absorption properties significantly and renders them interesting substructures in the construction of organic photoactuators. Specifically, as building block of molecular organic photoswitches and motors, they can be used to efficiently convert the energy applied by means of a light stimulus into motion on the molecular scale. Here, we will discuss the application of indole and its derivatives as core structures in various organic photoactuators and highlight the impact of this structural motif with respect to its isosters.*

Contents

1. Introduction

Indole and its derivatives (Figure 1A) represent one of the essential and versatile cores that the synthetic organic chemist can exploit in their path towards the synthesis of a target molecule. The degree of aromaticity and increased electron-richness of indole compared to its isosteres benzofuran and benzothiophene are one of the key factors that allow multiple routes towards its selective functionalization.[1-3] Moreover, the *N*-atom in its structure provides a handle for easy derivatization and an additional site that assists its asymmetric derivatization.[4]

Indole derivatives are without any doubt privileged structures in medicinal chemistry and drug development. These scaffolds are indeed incorporated into a diverse range of molecules characterized by high potency towards a diverse set of biologically relevant targets.[5-11] This peculiarity might not come as a surprise to the reader, considering the ubiquity of indole moieties in many alkaloids, plant hormones, and several pharmacologically active compounds, as well as the essential amino acid tryptophan (Figure 1B).[5,11] The prominent role of indoles in biochemical actuators is equally matched by their preeminence as the core component of metal-free organic dyes. Introducing an indole derivative in a molecule can indeed modify the absorption properties of the molecule itself. Indigo, the overcrowded alkene dimer of 3-oxindole, is the archetypal indole-based derivative that revolutionized the pigment industry and the coloration of fabrics, due

to its broad, intense absorption in the visible range, with a band peaking at 440 nm.[12] Related structures, isoindigo and indirubin, among them compose the family of indigoid dyes represented in Figure 1C.

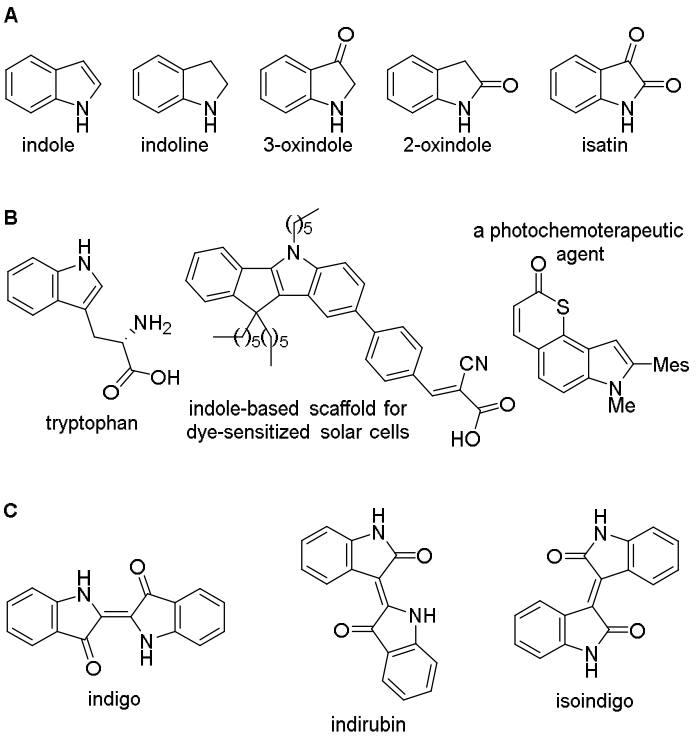

Figure 1. **A**. Structures of indole and its derivatives. **B**. Indole-based biologically relevant structures and an exemplarily indole-based scaffolded using in organic solar cells. **C**. Indigo and its structural isomers indirubin and isoindigo.

Among all the possible external stimuli, light possesses a fascinating flavor. Irradiation with an electromagnetic wave of a given frequency promotes the molecule to an excited state, an energetic *detour* that skips the ground state thermal barriers (Figures 2A and B).[13] Moreover, photons represent the perfect environmentally benign reagent because their action does not leave any trace in the reaction mixture.[14] The energy of the photons can be tuned to match the precise bandgap between the ground and excited states of the molecules while their nature can be exploited to achieve spatiotemporal resolution during a photochemical reaction. In this context, the natural electron-richness and the possibility to introduce further substituents on the N makes indole derivatives an attractive donor component in organic dye-sensitized solar cells.[15] Due to its reactivity upon irradiation, an indolin-2-one based compound was designed as photochemotherapeutic agent.[16]

One of the most fascinating transformations, that can be triggered by light, is the *E-Z* isomerization of double bonds (Figure 2C).[17] This reaction represents the cornerstone behind the concept of photochemically driven molecular motion. The study of artificial molecules able to interconvert between different forms upon light irradiation (photoactuators) dates back to the early 20th century with the discovery of the photochromism of the C=C and N=N bonds in stilbene and azobenzene (Figure 2C). Later, also other types of photochromic molecules, such as diarylethenes (DAEs, Figure 2C), which respond to light *via* an electrocyclization reaction, were discovered.[18] In contrast, fulgides,[19] fulgimides,[20] the spiropyran/merocyanine photochromic couple,[21] and donor-acceptor Stenhouse adducts[22] (DASAs, Figure 2C) exhibit more complex, multi-step photochemical isomerization mechanisms.

Upon irradiation, these photoswitches[23] (Figure 2C) can populate a metastable form which can be reverted to the initial isomer using another photochemical (P-type photoswitch) or thermal (T-type photoswitch) stimulus, depending on the substituents.[24] These transformations are accompanied by notable structural and electronic changes in the chromophore. The different properties of the metastable state in terms of geometry, electronics and thermal stability can be exploited by the chemist to induce changes in the properties of the molecule and on its environment upon light irradiation. The introduction of point and helical chirality elements in the photoactive molecule allowed the development of light-driven unidirectional molecular motors based on overcrowded alkenes in 1999 (Figure 2B).[25] With this particular example, a succession of photochemical and thermal events imparts directionality to the C=C isomerization, a significant mechanistic advantage compared to the otherwise stochastic nature of the motion in photoswitches.

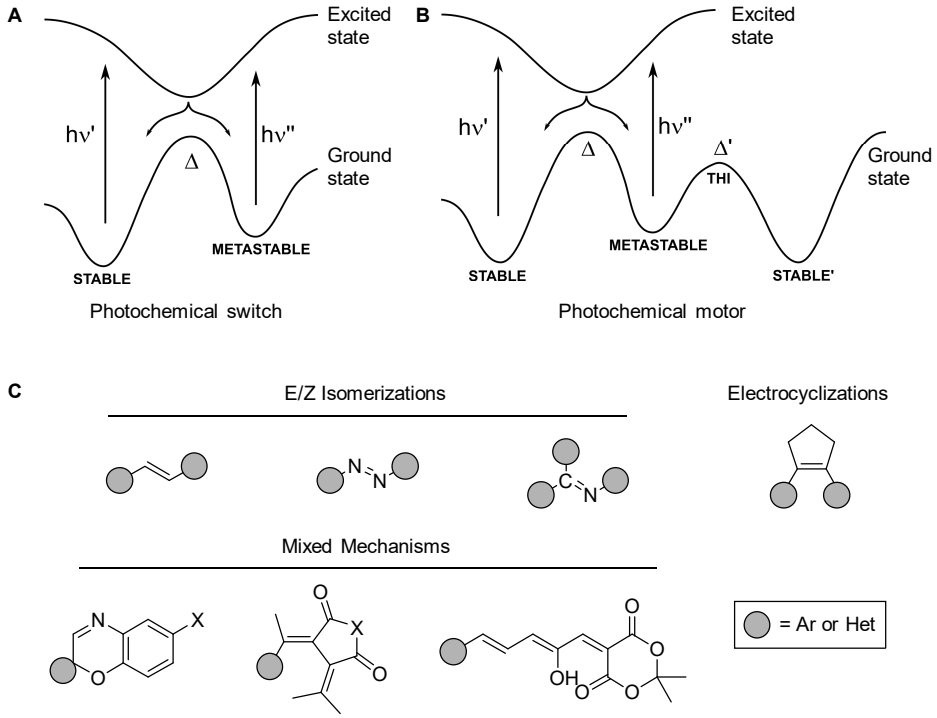

Figure 2. **A**. Simplified potential energy diagram of a photoswitch reversibly isomerizing between its thermodynamically stable and photochemically generated, metastable isomer upon irradiation with different light stimuli. **B**. Simplified potential energy diagram of a molecular motor characterized by a thermal ratcheting step. The thermodynamically stable state isomerizes photochemically, generating the metastable isomer. In this design, the metastable form can revert thermally to the initial stable isomer or, due to introduction of point and helical chirality elements into the molecular structure, isomerize to a second stable state (STABLE') *via* thermal helix inversion (THI) through a lower thermal barrier. **C**. Representation of different prototypical molecular switches and motors associated with the respective photochemical isomerizations: *E/Z isomerizations* around C=C, N=N, and C=N bonds as present in stilbene, azobenzene, and imine-based photoswitches; *electrocyclization*s, as represented by diarylethenes[18] (DAEs); photoswitches that isomerize in more complex, multistep mechanisms such as the spiropyran/merocyanine photochromic couple,[21] fulgides,[19] fulgimides,[20] and donor-acceptor Stenhouse adducts[22] (DASAs).

This chapter will discuss the application of indole derivatives as ideal core motifs in the design of various classes of photoswitches and motors, with particular attention to the one reported in Figure 2C. We will discuss their photophysical properties while focusing on their photochemical and thermal isomerization behaviour. We will highlight the peculiarities that characterize these heteroaromatic compounds compared to the homoaromatic parent molecules, showing the potential challenges and applications of this scaffold in building photochemical actuators.

2. Indigo and indigoid photoswitches

2.1. Indigo, indirubin, and the peculiarity of isoindigo

In the second half of the 19th century, the structure of indigo was determined by Nobel laureate Baeyer, who later also developed the synthesis of the dye from *ortho*-nitrobenzaldehyde **1** and acetone **2** (Scheme 1) together with Drewsen.[26,27] Later, Heumann used **3** as starting material to synthesize indigo under alkaline conditions and heat. The formed intermediate **4** readily decarboxylates under the reaction conditions and condensates to indigo. Shortly after Heumann presented his approach, Pfleger demonstrated a similar protocol using *N*-phenylglycine **5** as starting material, which is cyclized to indoxyl **6** and spontaneously condensates to indigo. The procedure developed by Pfleger nowadays still represents the lion's share of the industrial synthesis of indigo.[28]

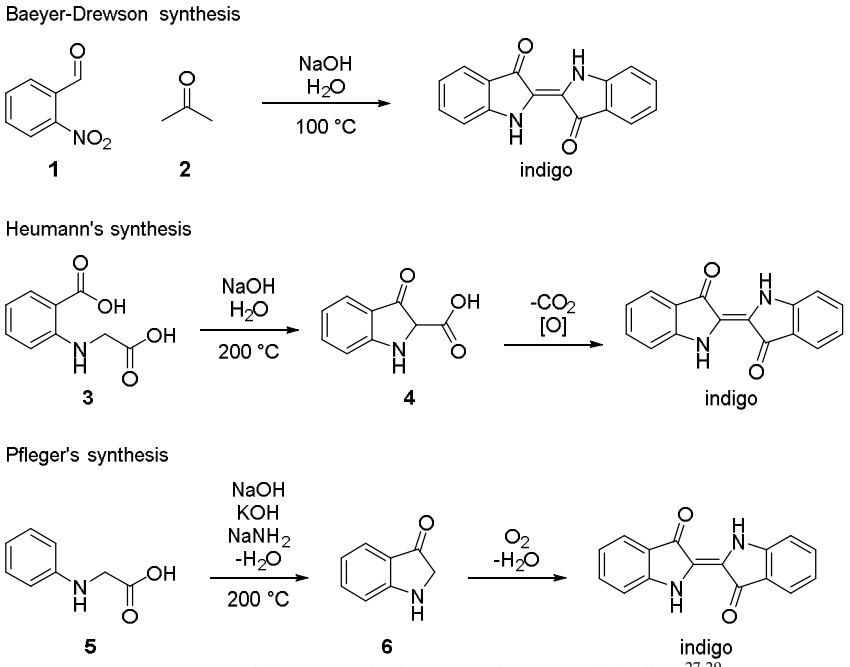

Scheme 1. Different synthetic approaches towards indigo.[27-29]

In contrast to the related thioindigo,[30-33] the photochromism of indigo was not extensively studied until recently.[34] This discrepancy is mostly related to the predominant de-excitation pathway of the excited state of indigo, an excited state intramolecular proton transfer (ESIPT) (Scheme 2A), which leads to the high photostability of the popular dye.[12,35,36] Due to the small energy gap between the ground state and excited state,[37] the extended indole scaffold of indigo can be addressed with green to red light which drives the $S_0 \rightarrow S_1$ transition. After having populated the excited state, the molecule can access a conical intersection (CoIn) that drives the ultrafast nonradiative decay of the molecule to the ground state along the coordinate of the single *N*H proton transfer (Scheme 2A) to the neighbouring ketone, obtaining the corresponding mono

enol form.[12,36] On the other hand, *N*R functionalized indigos avoid the ESIPT pathway and are known to undergo *E*-*Z* photoisomerization with red light since the 1950s.[38] The alkylated indigos possess negative photochromism, consequently the absorption spectrum of the metastable isomer is hypsochromically shifted compared to the stable one, in this case of around 100 nm in the blue (from 546 to 438 nm in di-^{t}Boc indigo), and show switchable fluorescence.[35] However, the thermal lifetimes of the metastable *Z* isomers of compounds functionalized with electron neutral alkyl derivatives are very short (<5 s) at ambient conditions and hence, not suitable for many applications necessitating bistable photoswitching, *i.e.* a lifetime of the metastable state usually longer than the hour range.[35,39-41]

More recently, the range of *N*-substituents was further extended and the associated photophysical and photochemical properties were systematically studied.[34,42] In particular, functionalization with electron withdrawing aryl substituents on the indolic nitrogen resulted in indigo derivatives with thermal half-lives in the minute to hour range, extending significantly the potential applications of this category of photoswitches by stabilizing the metastable form of the switch. ^{t}Boc functionalization of the nitrogen increases the lifetimes to >120 min.[35] These compounds differently substituted at the nitrogen retained the inherent visible-light responsiveness of indigo derivates and are able to stabilize pronounced structural changes upon photoisomerization.[34] Hecht and co-workers studied the tunability of the photochromism in the indigo family (Scheme 3 for different approaches to post-functionalize indigo to obtain bis-alkylated **7**, bis-arylated **8**, and mixed compounds **9**), focusing the attention on the modifications of the nature of the nitrogen substituents to vary the thermal stability of the *Z*-form (Scheme 2B).[34] An interesting finding that underscores the potential of this switches is the relatively limited effect of the substituents on the photophysical properties (in terms of wavelength associated with the maximum of absorption of the stable and metastable forms and respective absorptivities) compared to the more pronounced effect on the thermal back isomerization rates. As an example, bis-arylation on the N with two *p*-substituted MeO affords an absorption of 645 nm of the *E*-isomer and 599 nm of the *Z*, with a thermal half-life of the latter of 58 s. Conversely, the *E*-indigo bis-arylated with two phenyls with NO_2 in para position absorbs with maximum at 620 nm and, when irradiated, the maximum of absorption shifts at 577 nm. This *Z*-form is stable at room temperature with half-lives of 408 min.[34] Interestingly, also the distribution of the two isomers when the so-called *photostationary state* is reached favour the compound decorated with electron-withdrawing groups. In the former, only 52% of the mixture is characterized by the *Z*-form, while in the latter the photostationary distribution is enriched with 80% of the metastable isomer.

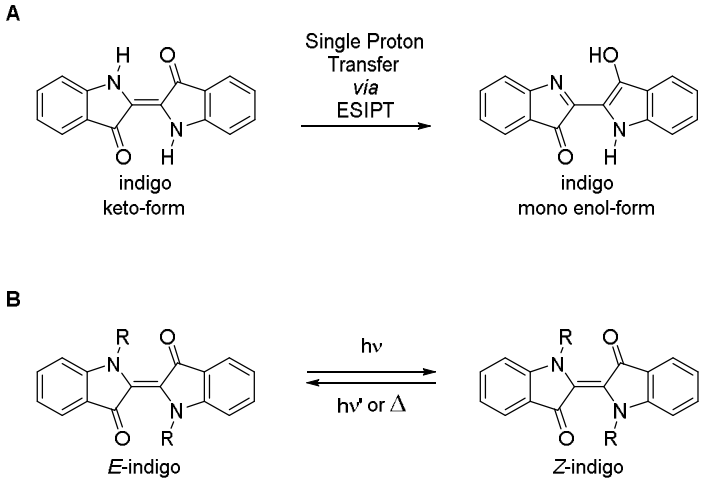

Scheme 2. A. Proposed mechanism of the excited state intramolecular proton transfer (ESIPT).[12,36] **B**. General representation of the photochemical isomerization of differently *N*-functionalized indigos.

On the other hand, mono-arylated indigos exhibit thermal lifetimes in the minute range and the unsubstituted *N*H can be used to fine-tune the thermal stability of the metastable form by the amount of water present in solution, which facilitates an intramolecular relaxation pathway.[43] The peculiar role of the *N*H in tuning the lifetime of the metastable form of the photoswitch have been observed also in other classes of indigoid and more generally indole-based photoswitches (*vide infra*).

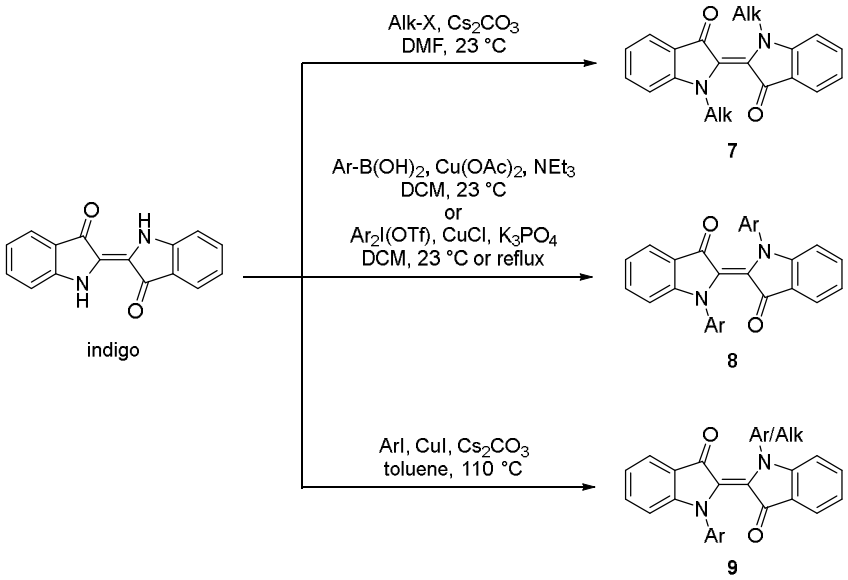

Scheme 3. Various strategies to achieve *N*-functionalization explored by Hecht and co-workers.[34]

Indirubin was first synthesized alongside with its constitutional isomer indigo as a side-product during the synthesis of the latter.[44] Specifically, the common intermediate indoxyl **6** can be easily oxidized to isatin **10** under the same reaction conditions (Scheme 4A). Isatin **10**, thanks to the more reactive carbonyl in benzylic position, can then undergo a condensation reaction with a second indoxyl molecule to result in indirubin instead of the (desired) indigo. As the parent compound, indirubin is strongly coloured and absorbs readily in the visible range of the electromagnetic spectrum (561 nm in xylene).[45] Another similarity is its high photostability, which can possibly be ascribed to an ESIPT deexcitation pathway, analogous as the one observed in indigo.[46] Consequently, alkylation of both *N*H units prohibits that pathway and facilitates the reversible photoisomerization of the central double bond, as reported very recently by Dube and coworkers.[47] The authors of the study point out that to allow photochemical isomerization, at least the *N*H proton of the indigo fragment needs to be alkylated. The *N*-functionalization of the isatin half is more independent from these requirements, as it can be derived from its position relative to the C=O group of the indoxyl moiety, which does not allow for a facile intramolecular interaction.

The different indirubin derivatives studied were synthesized from 3-acetly indoxyl **13** and differently substituted isatins (*e.g.* **11**) (Scheme 4B and C), reacted as is or previously functionalized *via* nucleophilic aromatic substitution (compound **12**) (Scheme 4B) to afford compound **14**. The latter were alkylated with *n*-iodopropane **15** under basic conditions to result in the final series of compounds **16** (Scheme 4C), which were studied regarding their photophysical and photochemical properties. Propylation (or in general alkylation, preferably with branched alkyl chains) allows for better solubility of these photoswitches in organic solvents.

Both isomers of indirubin exhibit absorption in the green-red region (between 500 and 700 nm). In contrast to the parent indigo, the UV/Vis absorption does not change dramatically, influencing the percentage of the other isomer that can be populated upon light irradiation.

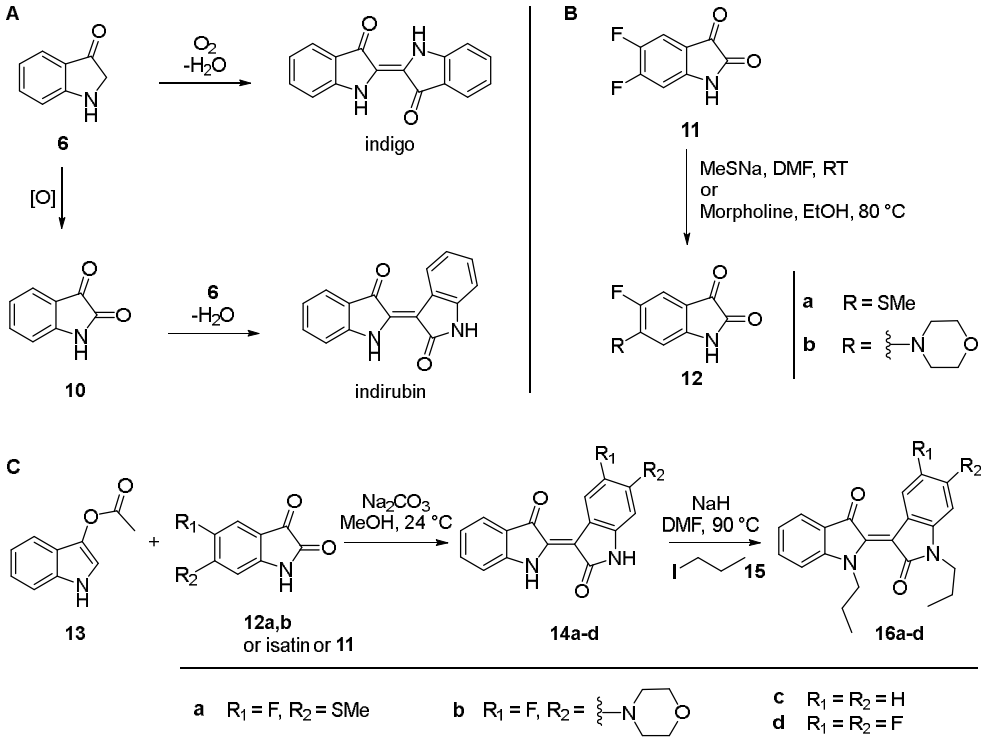

Scheme 4. A. Classical synthesis of indirubin as a side-product of indigo by Baeyer and Emmerling.[44]
B-C. Synthesis of substituted isatins and indirubins to make photoswitchable derivatives by Dube.[47]

When unsubstituted indirubin is considered, the thermally more stable *Z* isomer can be irradiated with 625 nm light to form the metastable *E* form. This transition is characterized by negative photochromism, due to the hypsochromic shift of the absorption maximum (Scheme 5A) (*e.g.* for unsubstituted indirubin the absorption maximum shifts from about 590 nm to 575 nm). In addition to the very similar absorption spectra, the *E* form can be enriched only up to 46% in toluene also due to the higher quantum yield of the competing *E*→*Z* isomerization (0.8% *Z*→*E* vs. 1.8% *E*→*Z*). In contrast, in DCM, the metastable form can be accumulated up to 62%. In this case, selective *E*→*Z* isomerization can be triggered either with 425 nm light, giving the thermally favour *Z* isomer up to 90%, or occur thermally in 2.6 min-2.7 h at 20 °C, depending on the solvent and on the nature of the substituents on the nitrogens of indirubin.

The authors employed a supramolecular approach to increase the amount of the *E* form that can be accessed by photoisomerization. Using the fully *N*H substituted compound, the photostationary distribution can be significantly increased by adding Schreiner's thiourea organocatalyst (STC), which preferentially interacts with the metastable isomer *via* H-bond interactions (Scheme 5B and C). As a result, up to 84% of the *E* isomer can be formed upon irradiation with 625-650 nm. Adding STC, the system responds with positive photochromism, because the absorption spectrum of the *E*-indirubin-STC complex is bathochromically shifted up to the NIR region. Consequently, photochemical *E*→*Z* isomerization can be achieved with 730 nm light, rendering indigo a photoswitch operating fully with red-light. The better performance of the supramolecular system relies mainly on the photoisomerization quantum yields, mostly the one of the *E*→*Z* reaction, being affected by the presence of STC (0.7% *Z*→*E* vs. 0.4% *E*→*Z*) as the band separation at the wavelengths of irradiation is not pronounced. The *E*→*Z* back-isomerization can additionally be addressed with blue light and thermally allowing quite some flexibility for tuning of the overall system for various applications while replying exclusively on visible light and/or heat (Scheme 5A).[47]

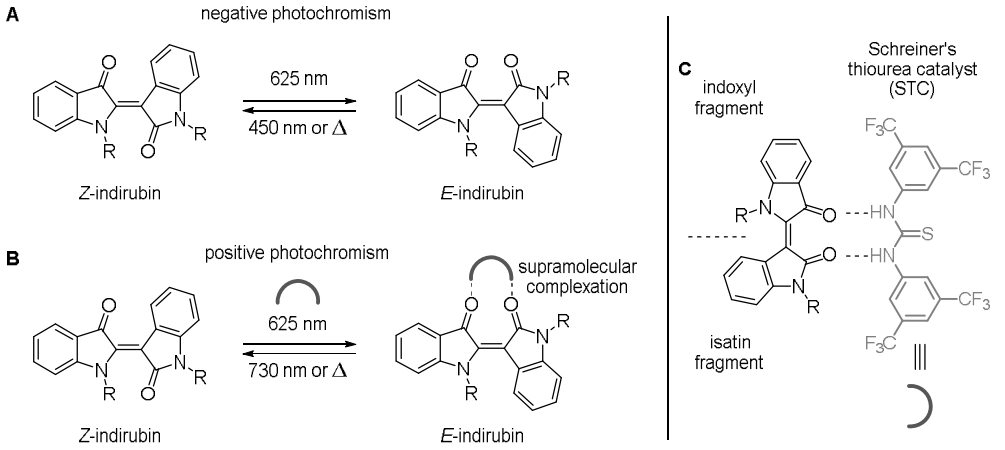

Scheme 5. *N*-functionalization of indirubin and its supramolecular complexation by Dube and coworkers.[47]

Similar to indigo and indirubin, also their structural isomer isoindigo (Scheme 6A) bears a central, overcrowded alkene that is simultaneously a stiff-stilbene derivative, and is intrinsically absorbing in the visible region of the electromagnetic spectrum.[48] The molecule is used to build optoelectronic materials[49-51] and of interest for biological applications.[52,53] As the parent dye, isoindigo is known to be photochemically extremely stable. However, alkylation or arylation of isoindigo does not facilitate photoswitching. This chemical functionalization, which proved successful in avoiding competing ESIPT pathways in indigo and indirubin (*vide supra*) is not effective in this case.

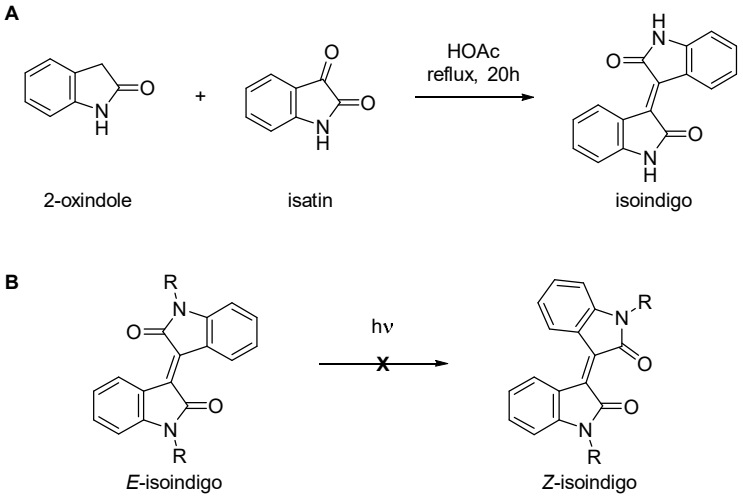

Scheme 6. A. Condensation of 2-oxindole and isatine to isoindigo.[48] **B**. Excitation of the thermally stable *E*-isoindigo does not result in photoisomerization despite *N*-functionalization, but in ultrafast relaxation *via* intramolecular singlet fission.[54]

The participation of this intramolecular de-excitation reaction in isoindigo can be indeed confidently ruled out, due to the relative position of the C=O and *N*H groups, which cannot interact at the excited state due to the prohibitive distance. On the other hand, the authors of a recent study postulate the possibility of an intramolecular singlet fission pathway leading to ultrafast decay in the ps time scale. The authors identified

the spectral signature of the ^{1}(TT) state of isoindigo in solution thanks to its similarities with the transient absorption spectrum of its triplet state, obtained by sensitization (Scheme 6B).[54]

2.2. Hemiindigo and the related hemithioindigo

Hemiindigo (HI) (Scheme 7A) is also known as azanaurone[55] and consists formally of half indigo (an indoxyl moiety) and half stilbene connected *via* a central C=C axle, about which the molecule can be photochemically and thermally isomerized.[56] The synthesis toward HI starts as the ones of the structurally related indiribin (*vide supra*) and phenylimino indolinones (PIOs *vide infra*) from 3-acetly indoxyl **13** (Scheme 7B). The compound is treated with NaOH and then condensed with benzaldehye **17**, resulting in the unfunctionalized HI **18**.[57] The compound can be further modified at the indolic nitrogen by either alkylation with alkyl iodides or by palladium-mediated cross-coupling reactions with aryl bromides to yield functionalized His **19** (Scheme 7B). The so formed HIs exhibit an absorption maximum around 450 nm showing that replacing one of the two benzene rings in stilbene with the indole derivative leads to a pronounced bathochromic shift in the absorption properties of the switch (stilbene absorbs at 295 nm).[58] The UV/Vis absorption profile can be further tuned by attaching electron-donating substituents in *para*-position of the stilbene moiety and by the polarity of the solvent. More polar solvents induced the stronger shift, to eventually result in green-light responsive switches.[56]

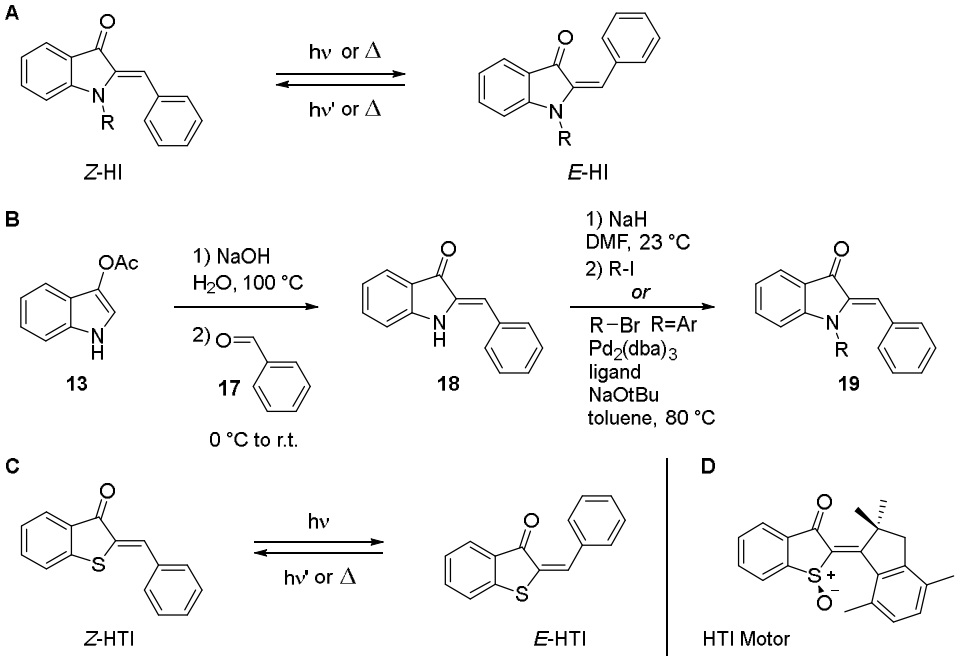

Scheme 7. A. The two photoisomers of hemiindigo (HI). **B**. Synthesis of (substitutes) HI. **C**. The two photoisomers of hemithioindigo (HTI). **D**. Example of a HTI based molecular motor.

The thermodynamically favored *Z* form shows positive photochromism upon irradiation which is accompanied by formation of the *E* isomer. The *E* form absorbs typically between 500 nm and 600 nm and can be switched back to the *Z* photochemically using light of a suitable wavelength.[57] The photoinduced interconversion between *E* and *Z* isomer proceed close to quantitative in both directions, independently from the polarity of the solvent, when moving from toluene, THF, to DMSO. The compound shows little to no fatigue upon multiple series of photochemical isomerization cycles between the two isomers.[56,57] Envisioning applications in a more biological scenario , HI can be readily (photo)isomerized achieving up to

80% of the metastable *E* form in water and organic solvent-water mixtures.[59] The aqueous medium, however, lowers the band-separation between the two photoisomers.[59,60] In contrast to indigo derivatives (*vide supra*) or azoindoles (*vide infra*), the thermal stability of the metastable isomer in *N*H-containing HIs is less affected by polar protic solvents. The metastable form exhibits thermal lifetimes in the range of several days.[59] Attaching other substituents than H onto the indolic nitrogen causes the two photoisomers to become energetically very similar. Consequently, heating of the pure *E* or the pure *Z* form results in a mixture of both (however, with extremely high thermal barriers that makes both forms stable with half-lives of about 83 years) (Scheme 7A).[57,61]

Despite being outside the scope of this review, we would like to make the reader aware that replacing the nitrogen with sulfur results in hemithioindigo (HTI) (Scheme 7C), half thioindigo and half stilbene. These compounds are emerging in various applications in recent years.[56,62-64] In contrast to the previously discussed HI, HTI clearly favours a thermodynamically stable isomer, the *Z*, over a metastable one, the *E*. The absence of the indolic nitrogen required more elaborate synthetic techniques for functionalization of the bicyclic moiety than simple *N*-alkylation and additional substituents are often introduced in the benzo-moiety *para*-position to the sulfur.[56] Partial oxidation of the sulfur itself allows to introduce an element of chirality in close proximity to the photochemically active C=C[65] and facilitated the development of an unidirectional multistep photochemical actuator, *i.e.* a molecular motor (Scheme 7D).[24] We refer the interested reader to works focusing principally on these compounds.[65-69]

2.3. Arylliminoindolinones

Aryliminoindolinone photoswitches were only recently identified as photochemical switches. They were designed starting from the with iminothioindoxyl (ITI) (Scheme 8A) photoswitches, which on the other hand were derived from the previously introduced HTIs. ITI, substitutes one the CH of the rotating axle with a nitrogen, making ITI a derivative that formally connects a hemithioindigo half with azobenzene. Analogously to HTI, ITI exhibits a thermodynamically stable *Z* (blue-light addressable) and a metastable *E* isomer. One of the peculiarities of the system is the marked difference in absorption maximum between the two photoisomers.

The *E* form is bathochromically shifted of about 100 nm, compared to the *Z*, allowing it to absorb green-orange wavelengths. Replacing the C=C bond in HTI with a C=N bond in ITI allows the *E* form to thermally access a nitrogen-inversion pathway with significantly lowered barriers compared to the rotation coordinate of the C=C bond.[70] This modification resulted in thermal lifetimes in the millisecond range.[70] The inversion-rotation dichotomy can be selectively enforced by protonating the C=N nitrogen inducing a change in thermal pathway affording both longer thermal $E \rightarrow Z$ isomerization times as well as a bathochromic shift in the UV-Vis absorption spectrum.[71] Replacing the thioindigo half of the switch by the analogous 2-oxindole motif allowed for swift functionalization at the indolic nitrogen (Scheme 8B). The synthesis proceeds from the commercial acetylated compound **20** which can be functionalized at the nitrogen by means of acetic anhydride. Deprotection of the oxygen of compound **21** forms the indoxyl derivative **22**, which can react with nitrosobenzene to afford quantitatively phenylimino indolinone (PIO) (Scheme 8B and C).

The indoxyl nitrogen provides a handle for extra functionalization and a way to tune the steric properties of both photoisomers, to ultimately control their relative stability. Indeed, increasing the steric bulk from a sulfur atom to the *N*-acetyl group allowed to invert the relative thermal stability of the two isomers, *E* and *Z*. This effect is a consequence of the net destabilization of the *Z* form, due to the increased steric demand of the Ac substituent. The substitution, however allowed to simultaneously retain the electronic properties of the respective isomers, but inverted photochromism compared to ITI. In particular, PIO is green-light responsive and showed a hypsochromic shift upon light irradiation.[72] The metastable isomer exhibited a thermal lifetime in the μs-range, which could be detected by means of nanosecond transient absorption spectroscopy. Substitution of the phenyl group with para substituent allowed to modulate the lifetime of the thermal step, with electron-withdrawing groups accessing faster isomerization rates thanks to the stabilization of the partial negative charge present on the imine nitrogen.[72] This particular electronic feature was used as a way to probe the nature of the thermal transition state in PIO, which was attributed to an inversion pathway as in ITI and in imines.

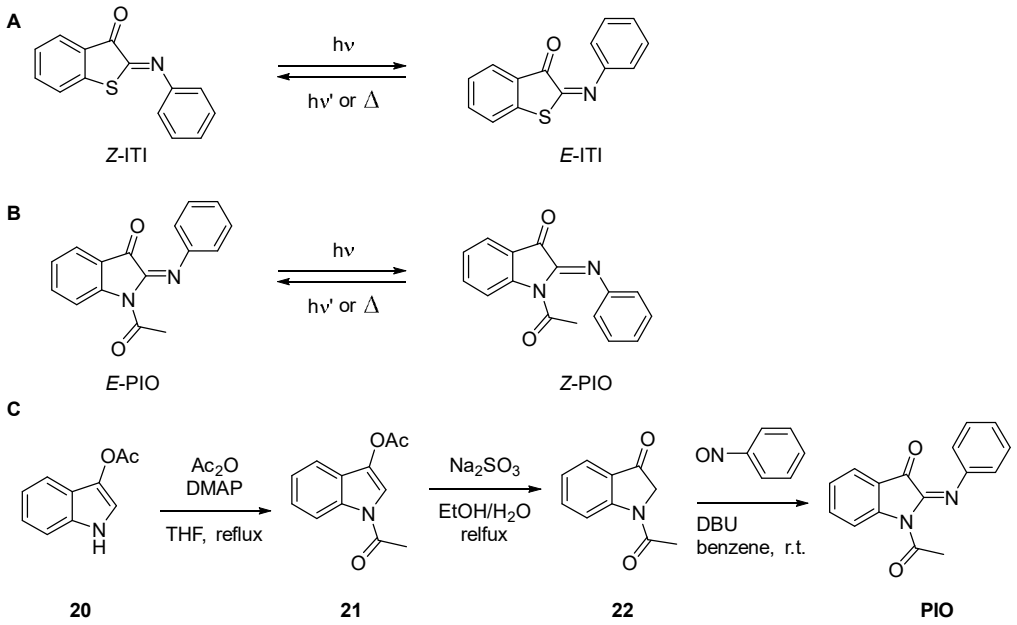

Scheme 8. **A**. (Photo)isomerization of Iminothioindoxyl (ITI). **B**. (Photo)isomerization of phenyliminoindolinone (PIO). **C**. Synthesis of PIO.

3. Feringa-type molecular motors based on oxindoles

The emergence of molecular machines as a tool to harness the energy of the photons and produce a directionality in the motion of a molecule at the nano-scale was very recently recognized with the 2016 Nobel Prize for Chemistry.[73] Molecular rotary motors are fascinating for their ability to drive the systems out from the thermodyamical equilibrium.[74] The unidirectional motion that characterize Feringa-type motors with a thermal ratcheting step (Figures 2B and Scheme 9A) has been employed in different fields,[75] spanning smart materials,[76,77] catalysis[78] and surface chemistry,[79] offering ample possibilities for new unexplored chemistry to be developed.[79,80]

Different designs of Feringa-type molecular motors have been synthesized and studied (often defined as generations) (Scheme 9A), however they are all characterized by some crucial features, which are, the presence (or emergence in case of meso compounds)[81] of one (or more) carbons possessing point chirality and the helical chirality granted by the overcrowded structures around the central double bond.[80,82] The combination of point and helical chirality allows for the formation of four different diastereomeric structures composing the rotational cycle of the motor, which can be populated sequentially *via* the alternating application of light and thermal stimuli (Scheme 9B), affording excited state photochemical *E-Z* isomerizations and so-called thermal helix inversion steps (Figure 2B). The applicability of such compounds is obviously related to the addressability of their core with visible light.

Very recently, the lower half of a second-generation molecular motor was substituted with an oxindole derivative, shifting the maximum of absorption of the overcrowded alkene at 370 nm, with a tail that can be excited with blue light.[83] These compounds can be easily accessed through a one-pot Knoevenagel-type condensation and the dimension of the ring connected to the alkene bond controls the speed of their thermal step. Despite these beneficial properties, the overall photoisomerization quantum yield of these structures was found to be extremely low (2-3%). To overcome this issue, we designed an oxindole molecular motor characterized by a more pronounced push-pull character **23** (Scheme 9C), to modify the electronic properties of the parent compound to resemble the more efficient, charged, biomimetic molecular switches developed by Olivucci and co-workers **24** and **25**. Adding two methoxy groups to the upper half of the oxindole motor, the quantum yields could be increased to 8-12%.[84,85]

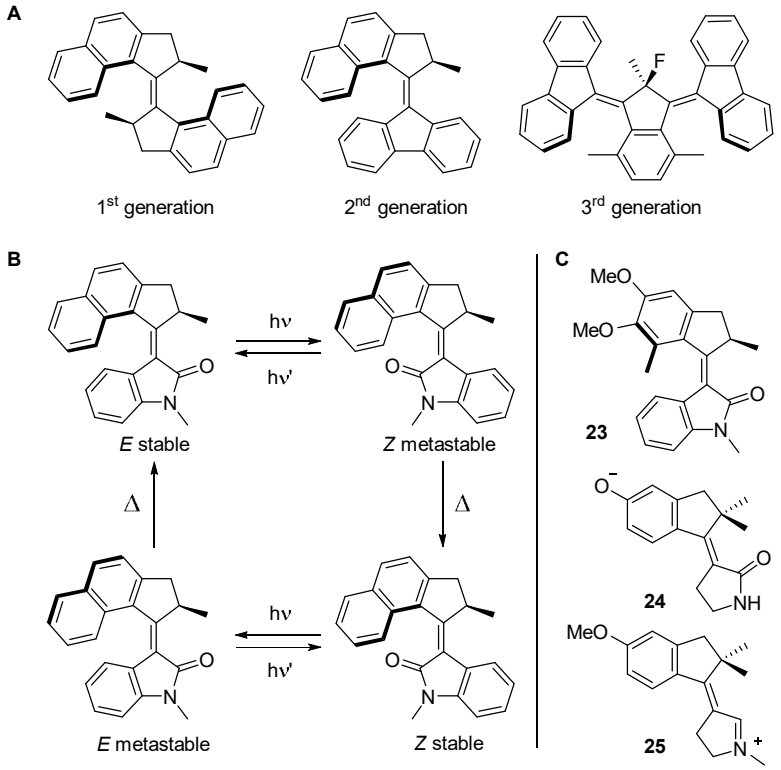

Scheme 9. A. Different generations of Feringa-type motors. 1st generation molecular motors are defined by the presence of two chiral carbons and helicity due to the steric clashes between the upper and lower halves. 2nd Generation molecular motors have only one chiral carbon and the helicity of the structure. 3rd generation molecular motors possess a meso carbon on a central moiety, attached to two fluorenones with the opposite helicity. The isomerization of one of the two fluorenones inverts the helicity of the structure, desymmetrizing the molecule and allowing unidirectional rotation.[80] **B**. Typical rotational cycle of a Feringa motor, here represented using an oxindole-type motor. The *E* stable state (a folded overcrowded alkene) isomerizes photochemically to the *Z* metastable state (a twisted overcrowded alkene). The latter form can invert its helicity *via* a thermal helix inversion process (THI) and form a more stable folded state (*Z* stable). The photochemical and thermal steps are then repeated to obtain the initial *E* stable *via* the *E* metastable intermediate. **C**. A push-pull oxindole motor **23** together with two biomimetic ionic switches **24** and **25**.[84]

4. Indole-based azo-photoswitches.

Azobenzenes have been studied as molecular photoswitches since the first half of the last century.[86] Only recently, heteroaromatic analogous have become increasingly more popular, due to the minimal structural modifications needed to impart huge changes in properties from the homoaromatic parent compound.[23,87] Among the different azo derivatives, we focused on the study of indole-based azoswitches, which have been synthesized with the N=N group attached to position 2, 3, 5, and 6 of the indole core.[88-91]

The photophysical and thermal properties of 2- and 3-phenyl azoindoles are strongly influenced by the heteroaromatic nature of the five-membered part of the indole bicycle to which the azo unit is attached.[88]

For instance, the UV/Vis absorption spectra of both compounds are 60-100 nm bathochromically shifted compared to azobenzene, an effect that usually requires elaborate substituent design, while in this case it is the electron-rich indole that allows this peculiarity.[23,87]

3-Aryl azoindoles (Scheme 10A), are attractive derivates due to the facile synthesis from indole **26** and a diazo compound **27** *via* azocoupling, which can access a wide range of compounds (Scheme 10B),[91]

allowing the introduction of further substituents to fine-tune the photophysical and (photo)chemical properties of the switches.[92] The synthesis of the other isomeric compounds proceeds *via* a Baeyer-Mills coupling between the corresponding amines **29** and **30** or ammonium **28** derivatives and nitroso benzene (Scheme 10C).

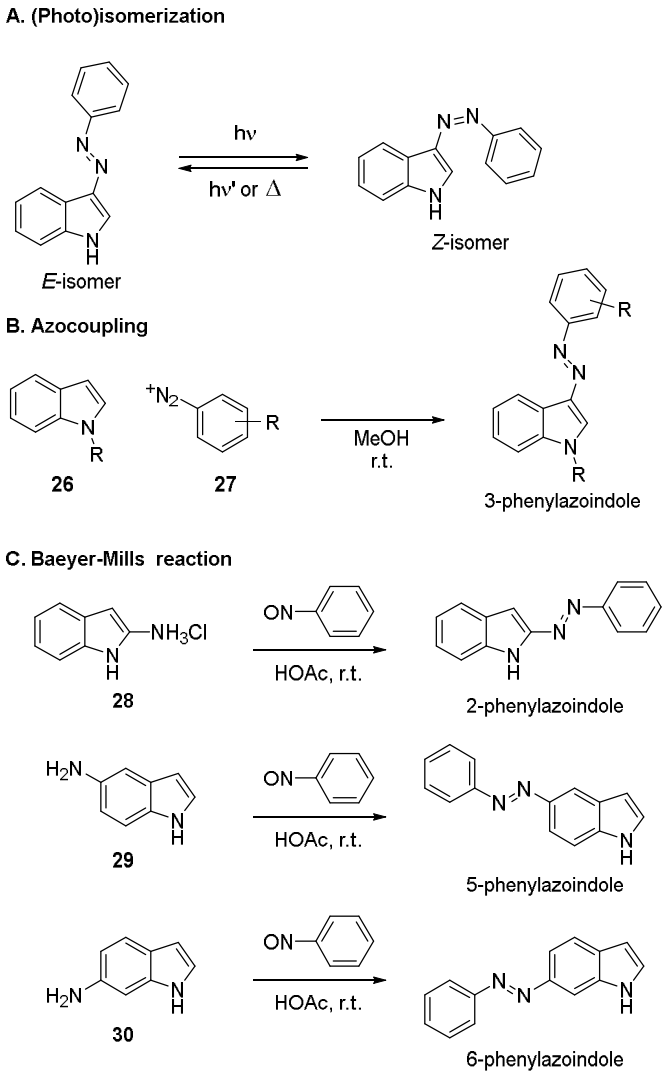

Scheme 10**. A**. (Photo)isomerization of 3-phenylazoindole.[89] **B**. Synthesis of various 3-phenylazoindeoles *via* azocoupling.[91] **C**. Synthesis of 2-, 5-, and 6-phenylazoindoles in a Bayer-Mills reaction.[88]

Irradiation of 3-arylazoindoles with UV to violet light induces photochemical *E*→*Z* isomerization. The isomerization about the N=N is accompanied with pronounced steric changes (Scheme 10A). While in classical azobenzenes the *Z* isomer assumes a helical conformation, in heteroaryl azobenzenes derivatives in which the azo unit is directly attached to a 5-membered ring, the *Z* form is T-shaped.[93] The thermal lifetime of the metastable *Z* isomers strongly depend on the individual derivative. The more classical 5- and 6-aryl azoindoles are thermally stable in the range of hours to days, while 2-arylazoindoles are sterically

destabilized in the *Z* form in which the phenyl moiety clashes with the *N*H function of the bicycle to result in extremely fast thermal *Z*→*E* isomerization kinetics in the low ns-range. The 3-arylazoindole derivatives are the most tunable ones and can access thermal lifetimes in the range of ns-days at ambient conditions depending on the particular substitution pattern and the used solvent. This characteristic is similar to other indole-based photoswitches, such as HI and parent indigo (*vide supra*). While 3-phenylazoindole, bearing an unsubstituted *N*H moiety, isomerizes within a few seconds in non-protic solvents from the metastable to the stable form, the isomerization rates significantly increase in protic environment.[89] This is due to the change in thermal isomerization pathway.[94] In protic media, like aqueous solvent (mixtures) or alcohols, the acidic *N*H proton can scramble onto the N=N double bond of the azo-function to result in a single bond between the nitrogens (Scheme 11). The so-formed *s-cis* hydrazone rapidly rotates about the N-NH single bond to the *s-trans* hydrazone and eventually tautomerizes back to the thermally stable *E* form. Both tautomerization steps are solvent-assistant intermolecular pathways.[89] Related observations have also been made for mono-arylated indigo[43] (*vide supra*) and this observation is a recurring phenomenon due to the nature of the indole core. Methylation of the indolic nitrogen in 3-azoindoles can enforce a change in the thermal isomerization pathway and leads to photoswitches with *Z* isomer lifetime in day-range.[89] Interestingly, the 2-functionalization leads to ns thermal isomerization lifetimes.[88]

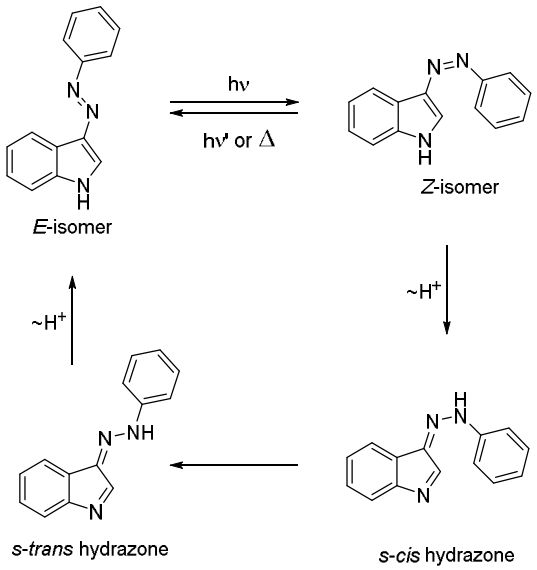

Scheme 11. Simplified representation of photochemical *E*→*Z* followed by thermal *Z*→*E* isomerization *via* tautomerization and hydrazone intermediate.

5. Diarylethenes

Diarylethenes (DAEs) typically consist of a hexatriene system with a bridged, central C=C bond to which two (hetero)aromatic rings are attached (*cf.* Scheme 5). [24,95,96] Irradiation with light between 300-365 nm, depending on the DAE derivative, induces an electrocyclization reaction involving the formation of a new bond that transforms the open (*O*) isomer into the corresponding closed (*C*) one (Scheme 12A).[95,97] The reaction proceeds according to the Woodward-Hoffman rules and is hence thermally forbidden, resulting to be irreversible up to high (>100 °C) temperatures. The thermal stability of the closed form is closely related to the energy associated with the loss of aromaticity of the (hetero)arene moiety[98] and the steric bulk around the newly formed bond in the *C* form.[96,98] For instance, some cyclopentene-bridge bis-indole-based derivatives are reported to be thermally unstable in the *C* form as the loss of the aromatic stabilization energy that indole provides to the *O* isomer is higher compared to, for instance, the more frequently used thiophene.[18,95,99] Moreover, the closed isomer of these compounds is somewhat labile to acids or in aqueous

media.[99] In contrast, unsymmetrically substituted derivatives, containing for example one (benzo)thiophene and one indole moiety are thermally more stable and more frequently employed than symmetrically substituted derivatives.[18] Especially, mono-indolyl maleimide-bridged DAEs were thermally stable over several days even in aqueous environment.[100] However, maleimide or maleic anhydride-bridged DAEs can typically not cyclize in polar (protic) medium due to a twisted charge-transfer state (Scheme 12B).[101]

As other DAEs, indole-based derivatives are typically colorless or pale yellow in the thermally stable open form, while the closed isomer is strongly colored with a broad absorption band in the visible range, the absorption maximum of which can be tuned by substituents into the orange to red region of the electromagnetic spectrum.[18] In particular, indole-based compounds often exhibit bathochromically shifted absorption profiles in their *C* forms with λ_{max} between 500-700 nm.[97,99,102-104] Moreover, they often show photoswitchable fluorescence[97,102,104] or photochromic FRET[105] and can even be reversibly isomerized in their crystalline form, due to the minimal geometrical changes imparted by the isomerization process.[102] By using two-photon excitation, unsymmetrically substituted indolyl DAEs could be addressed with light up to 820 nm.[103] The facile substitution of the indolic nitrogen and the strongly colored *C* isomers make indole-based DAEs interesting molecules for various applications and a sound starting point to develop related analogues based on azaindole[106] and purine to target photoswitchable nucleotides.[107]

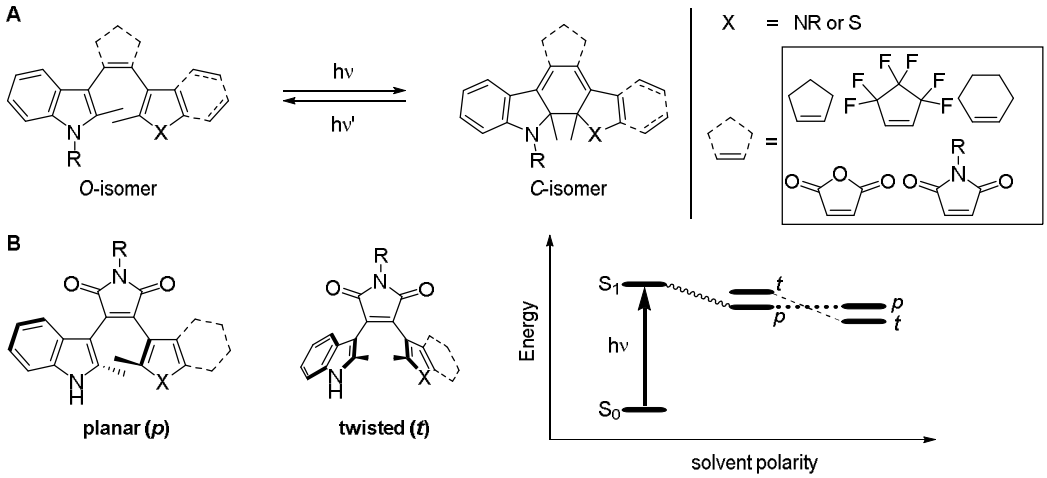

Scheme 12. A. Photoisomerization in indolyl-DAEs with different aromatic moieties and bridging units. **B**. Representation of the *O*-form in its planar (*p*) and twisted (*t*) conformation and their respective relative energies upon excitation in dependence of the solvent polarity.

The synthetic approach towards (indolyl)diarylethenes can be divided into two main routes. This selection typically depends on the nature of the central ethene bridge, being either is symmetrically[99,108] or unsymmetrically substituted. Symmetrically substituted DAEs can be synthesized *via* McMurry coupling as key step. Starting with indole **31**, two molecules are acylated with compound **32** to obtain compound **33**. The indolic nitrogen can be subsequently functionalized by alkylation **34** before the compound is cyclized using $TiCl_4$ and zinc as reducing agents, affording compound **35** (Scheme 13A).[99,108]

To obtain unsymmetrical DAEs, the same starting material can be coupled to bis-bromo maleimide **36** in a Michael-type addition-elimination sequence. The so-formed intermediate **37** can be alkylated **38** and then subjected to a Suzuki-Miyaura cross-coupling reaction to yield DAE **39** (Scheme 13B).[100]

Alternatively, 3-bromo thiophene **40** can be treated with butyllithium and the reacted with perfluoro cyclopentene **41** to yield mono-adduct **42**. This compound can be coupled with lithiated **43** in the same manner to achieve the unsymmetrical indolyl-DAE **44** (Scheme 13C).[102] More elaborated designs of indolyl-based DAEs or other DAEs often requires a similarly elaborate synthesis route, examples of which are discussed elsewhere.[95]

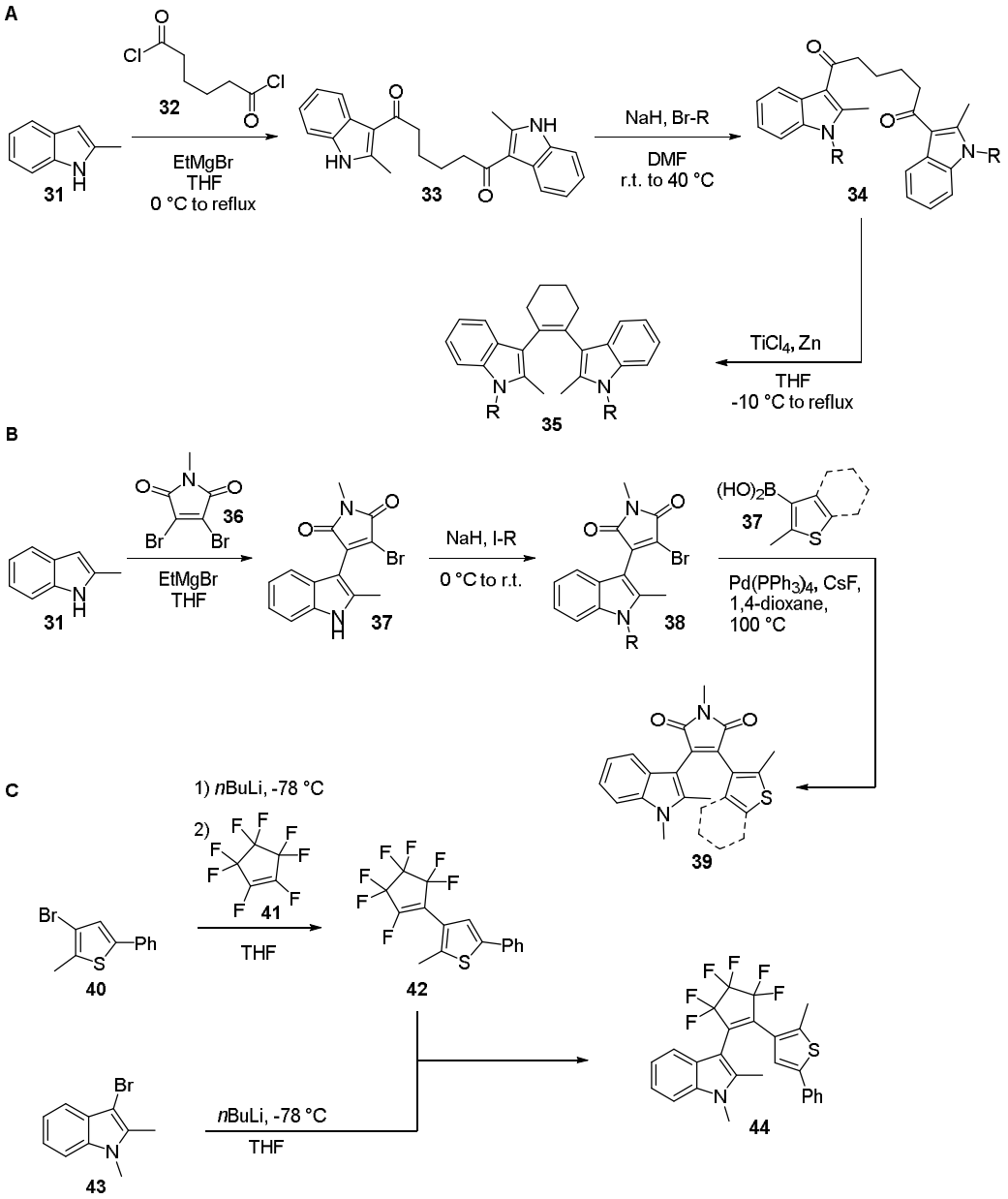

Scheme 13. A. Synthesis of symmetrically substitutes bis-indolyl ethenes *via* McMurry coupling.[99,108] **B**. Synthesis of unsymmetrically substitutes indolyl-based DAEs *via* Grignard followed by Suzuki-Miyaura cross-coupling.[100] **C**. Synthesis of unsymmetrically substitutes indolyl-based DAEs *via* stepwise lithium-halide exchange and nucleophilic substitution.[102]

6. Fulgides and fulgimides

As DAEs, fulgides and fulgimides exhibit a central hexatriene unit as the photochromic core structure (Scheme 14).[109] In contrast to the cyclic DAE photoswitches, two of the C=C bonds involved in the

cyclization are typically not part of a cyclic structure.[95,109] The two exocyclic double bonds are attached to either a succinic anhydride (when X=O, Scheme 14) in the case of a fulgide, or, for a fulgimide, to a succinimide unit (when X=NR, Scheme 14).[19] If these C=C bonds are unsymmetrically substituted, the photochemical isomerization about these bonds toggles between an *E* and a *Z* open form, a reactivity not possible for DAEs. Hence, fulgides and fulgimides are rendered multi-state photoswitches, involving a ring-open *E* and *Z*, and a *C* isomer.[110] However, the UV-Vis absorption spectra of both the *E* and the *Z* form are largely overlapping and hence, they cannot be addressed selectively.[111] Under irradiation with UV to violet light *E*-*Z* isomerization will occur when the bridging R-substituent is Me,[111,112] CF_3,[111,113] or COOH,[113,114] while larger substituents, such as *i*Pr,[111,112] *t*Bu,[111] or cyclic moeities[110,112] prohibit photochemical *E*-*Z* isomerization due to steric constraints. In this case, the two isomers can be separated chromatographically and only the *E* isomer can be used for the electrocyclization reaction to yield the *C* isomer, as the *Z* isomer cannot cyclize due to its geometry (for fulgides and fulgimides substituted in position 3 see Scheme 14A, for position 2 see Scheme 14B).[110]

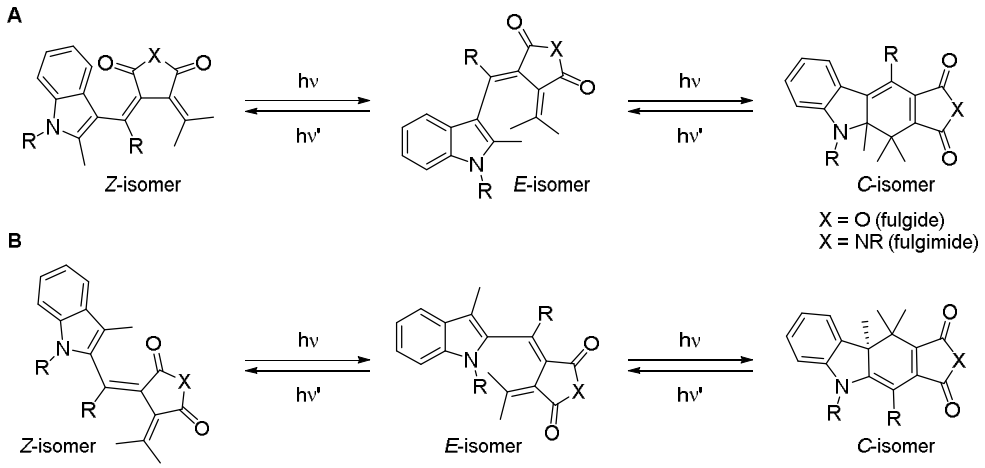

Scheme 14. A. Photoisomerization of indolyl fulgides and fulgimides condensed to the indole moiety in position 3. **B**. Photoisomerization of indolyl fulgides and fulgimides condensed to the indole moiety in position 2.

Indolyl-based fulgides and fulgimides can be synthesized from a suitably substituted indole **45**[98,10] (Scheme 15A) or **52**[115] (Scheme 15B). Indole **45** is acetylated in a Vilsmeier-Haack reaction to form compound **46** which is then *N*-functionalized to give **47**. For indole **52** these steps are typically inverted, with the alkylated product **53** that precedes the aldehyde derivative **54**. Both molecules, **47** and **54**, are then reacted with **48** in a Stobbe condensation to give the corresponding fulgides **49** and **55**, respectively. These compounds can be transformed into the analogous fulgimides substituting the O for an *N*R, by nucleophilic ring-opening of the anhydride with the desired functional group to be inserted (NH_3 for unsubstituted fulgimides, **50**, and H_2N–R for substitutes ones **51** and **56**).

The third double bond is typically part of the (hetero)aromatic ring, and its nature strongly influences the UV-Vis absorption spectrum. Consequently, indoles are often used due to their electron-rich nature and the possibility to introduce further substituents on the indolic nitrogen.[112,114,117] Besides indoles, also benzene,[118] (benzo)furan,[19,111,119] thiophene,[19,120,121] thiazole,[19] oxazole,[120] pyrazole,[19] and pyrrole[120] have been used.

The photochemically generated closed isomer in indolyl fulgides and fulgimides has a λ_{max} up to around 600 nm with the fulgimides being the more red-shifted derivatives.[19,111,112,120] The *C* form results to be thermally stable at elevated temperatures over several days,[19] and can be reversibly converted into the ring-open *E* isomer through irradiation with visible light.[111,121] As only the *C* isomer absorbs in the visible region of the electromagnetic spectrum, the *C*→*E* reaction typically proceeds quantitatively. The

photoswitching process in indole derivatives is robust and can be reversibly repeated over several cycles without any fatigue,[19,118,119,121] however, the efficiency of the reaction often varies between different solvents and if the photoconversion is the solid state.[111,121]

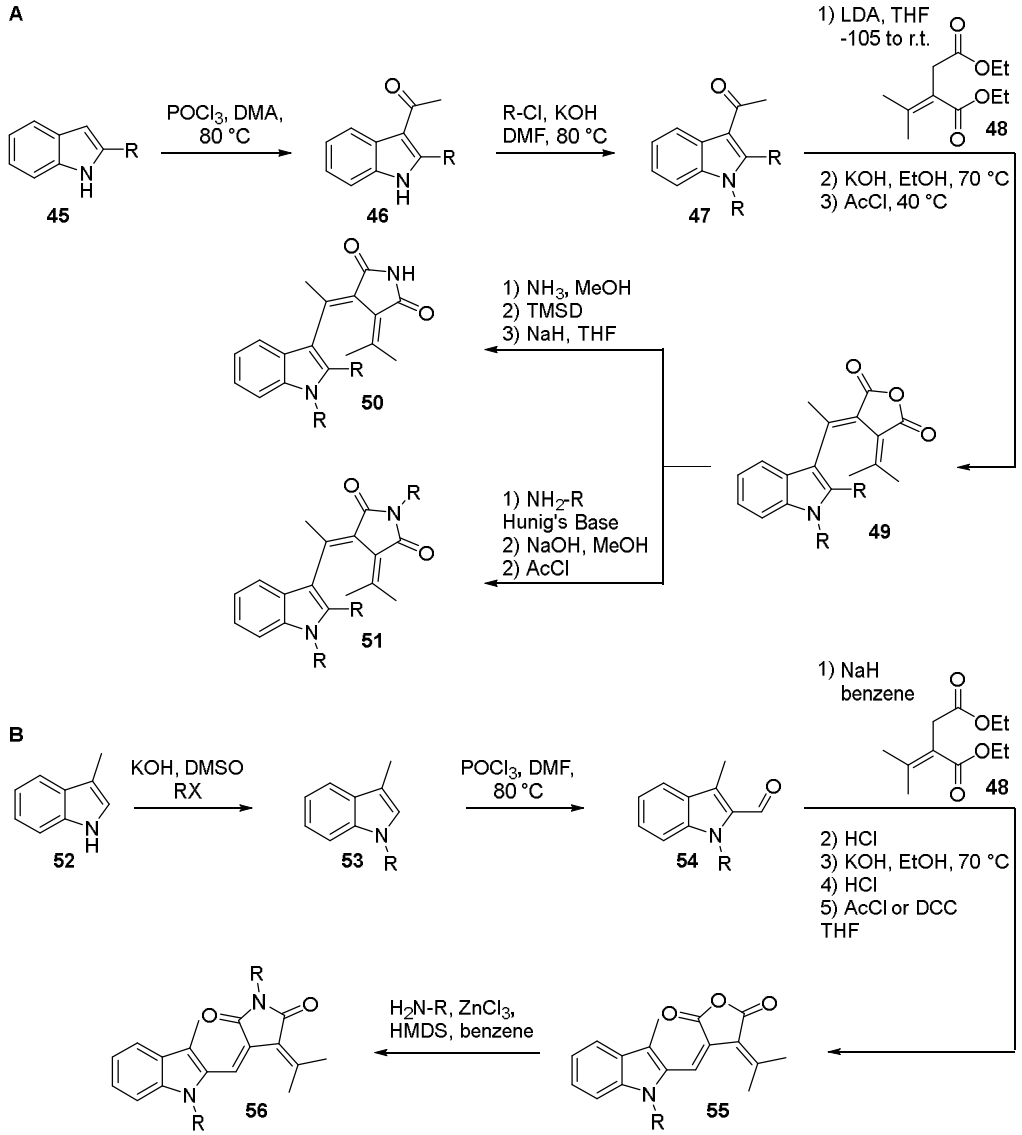

Scheme 15. A. Synthesis of indolyl fulgides and fulgimides condensed to the indole moiety in position 3.[112,116] **B**. Synthesis of indolyl fulgides and fulgimides condensed to the indole moiety in position 2.[115]

While fulgides can be hydrolyzed in alkaline solutions, fulgimides are usually more stable under such conditions.[19] However, in fulgimides with a R=CF_3 group attached to one of the exocyclic C=C bonds (***C*-57**), can be converted into a COOH group under basic conditions in water (***C*-58** Scheme 16A).[113] The so-obtained molecules can be reversibly photoisomerized between an open *E-Z* mixture and a *C* isomer

(***E*-58**, ***Z*-58** and ***C*-58** Scheme 16B).[113,114,122] However, under acidic conditions indolyl fulgimides with R=CO_2H can undergo a decarboxylation reaction to result in the non-photochromic ***C*-59** (Scheme 16A).[113]

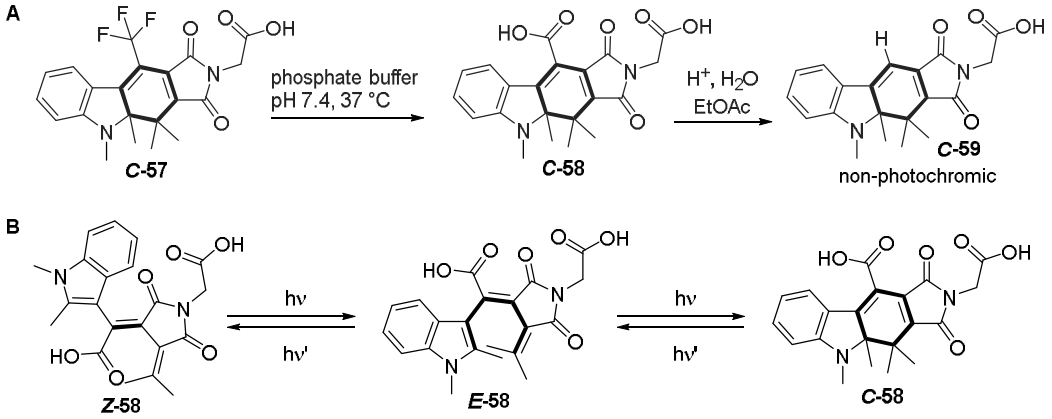

Scheme 16. A. Hydrolysis of ***C*-57** in phosphate buffer to yield the COOH-bridged ***C*-58**. While ***C*-58** can be photoisomerized in phosphate buffer (B), it is labile under acidic conditions and undergoes decarboxylation to ***C*-59**.[113] **B**. Photoisomerization of ***C*-58** in buffer.[113,114,122]

Suitably functionalized indolyl fulgides and fulgimides were used, for example, on surfaces,[123] in different biological applications,[119,124,125] as photoswitchable sensitizer,[126] as chiroptical switches in liquid crystal-based materials,[127] in all-photochromic logic systems,[128] or merged with other switches to construct multi-functional molecular units.[129]

7. Spiropyrans and merocyanines

Spiropyrans consist of an indoline and a chromene part, which have a spiro-junction in α-position next to the oxygen of the pyrene.[21,130] The spiropyran (SP)/merocyanine (MC) photochromic couple follows the same general mechanism as the previously discussed fulgides and fulgimides and can be cyclized *via* a 6π-electrocyclic reaction while the open isomer, the MC, can additionally undergo *E*-*Z* photoisomerization under irradiation with light of the same wavelength (Scheme 17A). The two open-form isomers, *E* and *Z*, can only be selectively addressed, when the phenolic O of the pyran is alkylated[131] or protonated.[132] In SP/MC, the hexatriene system contains at least one heteroatom, namely an oxygen in the pyran moiety, and, in the case of spirooxazine, an additional C=N double bond. Upon irradiation with UV-light, the pyrane C-O bond breaks and colourless SP can be converted into the more colored, open MC form.[21,133] The latter has a neutral, quinoidal and a zwitterionic form as the indoline N is in conjugation with the pyrene O.[21] In particular, electron-withdrawing substituents in para-position to the pyrane oxygen, such as the frequently used NO_2 group, stabilized the zwitterionic MC form.[21] The MC isomer is thermally metastable and has lifetimes that normally range between seconds and hours at ambient conditions.[134,135] The thermal lifetime can be tuned by substituents and by solvent, with organic solvents stabilizing the SP form better than aqueous ones, in which spontaneous ring-opening to the charges MC form is observed.[21,134,135] The (photo)isomerization is reversible over several cycles without fatigue in a variety of solvents[21,136] and can also be stimulated by other factors such as temperature (thermochromism), pH, or electrochemically.[21,133,137] Due to its response to multiple (orthogonal) stimuli, the switch is extensively studied and used in a wide range of applications.[21,133]

SP can be synthesized by alkylating 2,3,3-trimethyl-3H-indole **60** with a suitable alkyl iodide to obtain **61** (Scheme 17B). Upon treatment with piperidine, Fischer's base **62** can be formed and *in situ* reacted with benzaldehyde **63** to yield the desired spiropyran **64** upon elimination of water.

The SP/MC photochromic couple is frequently used in application where a prominent change in polarity is desired upon photoisomerization.[21,122] Thereby, the facile synthesis and the high degree of

flexibility that the indolic nitrogen offers in terms of functionalization *via* simple alkylation is an additional benefit of using the SPs in advanced applications.[21] As an example, the molecule can be used as photoacid generator (PAG), because the ring-opened MC form can easily be protonated on the ohenolic oxygen. Hence the bleaching of the MC is accompanied by a photo-induced ring-closure, where one proton per molecule of MC can be liberated in the medium (Scheme 17C).[21,140] Protonation with strong acid or photochemical ring-opening can invert the process.[21]

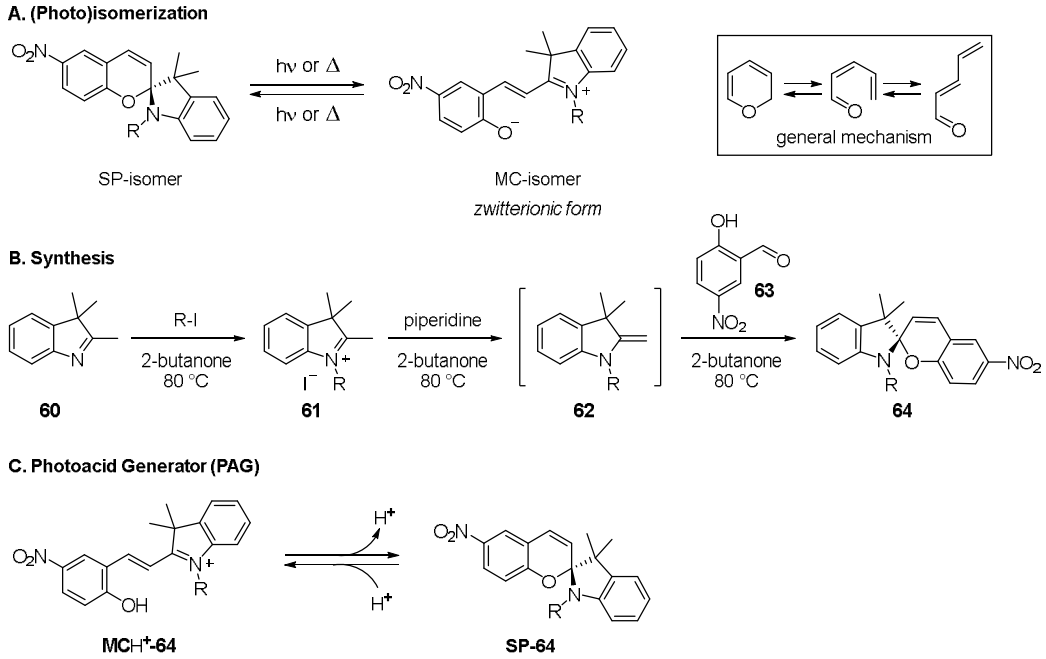

Scheme 17. A. Photoisomerization between the ring-closed SP-form and the ring-open zwitterionic MC form.[21] **B**. Synthesis of spiropyran **64**.[138,139] **C**. Photoisomerization of the zwitterionic MC **64** liberates H^+ and makes **64** a photoacid generator (PAG).[21]

8. Donor acceptor Stenhouse adducts

Donor-acceptor Stenhouse adducts (DASAs) are molecules consisting of a donor moiety, a triene bridge with an oxygen on C_2, and an acceptor moiety (Scheme 18A). Meldrum's acid, 1,3-dimethyl barbituric acid,[141] barbituric acid (Scheme 18B), or the strongly electron withdrawing carbon acids are used as the acceptor,[142] while either a dialkylamine[143] or secondary anilines, including various indolines, find application (Scheme 18A and C) as donor moiety.[141,142,144] Only recently, DASAs were reported to undergo reversible photoisomerization,[143] reason for which their popularity increased substantially in the photoswitch community.[22]

The synthesis of DASAs is straightforward and starts with a Knoevenagel condensation between furfuraldehyde **65** and a suitable acceptor moiety (Scheme 18C). In a second step, the furan is opened by reacting **66** with a nucleophilic nitrogen, originally with alkyl amines (1st generation DASA switches, Scheme 18D) or indoline derivatives for the 2nd and 3rd generation of DASA photoswitches (**67** and Scheme 18D).

The thermodynamically stable, linear form exhibits a UV-Vis absorption maximum in the visible range of the electromagnetic spectrum with λ_{max}=450-700 nm[22,146] and can be tuned by attaching further substituents or by solvent effects. Specifically, apolar solvents induce a bathochromic shift, while polar and non-polar ones have the opposite effect.[22,147] Also, the donor-moiety which is used in the molecule affects the absorption properties of the chromophore. Cyclic anilines, in particular indolines, induce a red-shift of

the main π–π* transition band up to the near infrared region of the spectrum, that can be further enhanced by introducing electron-donating substituents in *ortho* or *para* positions on the aromatic donor.[147-149]

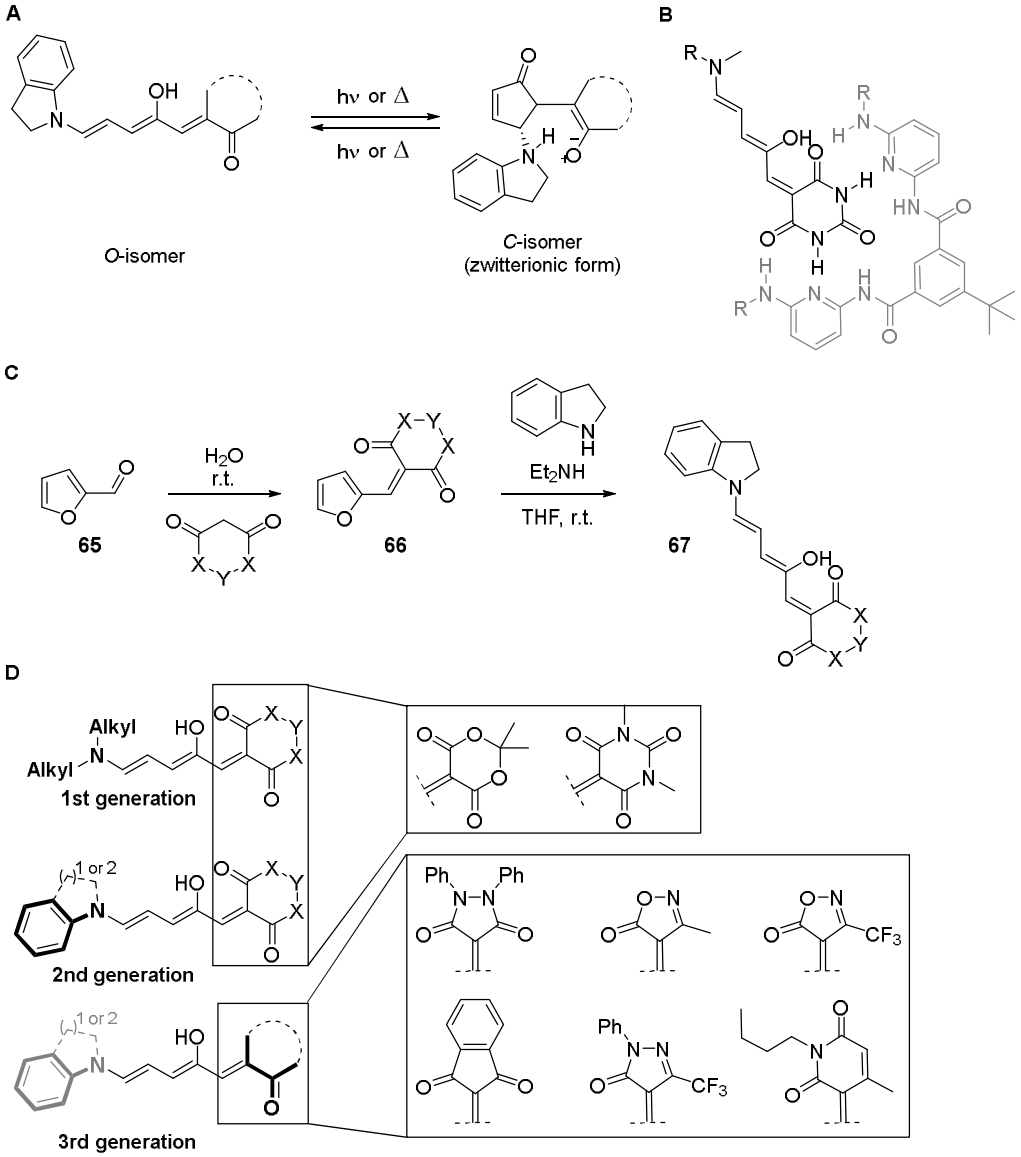

Scheme 18. **A**. Overview of the (photo)isomerization in DASA. **B**. General synthetic scheme of an indoline-based DASA photoswitch.[145] **C**. Synthesis of an indoline-based second generation DASA. **D**. Overview over the structural developments in DASA displaying representatives of the 1st, 2nd, and 3rd generations.[141,142,144]

Combined with the negative photochromism of DASAs, the compound hence is beneficial for several applications, for instance, in material sciences and biology as can be effectively isomerized with low-energy

light avoiding inner-filter effects.[150] These absorption characteristics derive from the fact that populating the π-π* transition rapidly leads to the bleaching of the push-pull substituted linear compound, with ensuing formation of new absorption bands that are derived from the formation of the cyclic form.[22] The cyclized form hardly absorbs at wavelengths longer than 300 nm and in the UV region shows only a limited band separation from the linear form.[143,148] Hence, recovery of the linear form *via* photochemical means is often impractical and consequently it is usually pursued thermally. Indeed, the closed form is thermally unstable and tends to revert to the open triene with lifetimes in the minutes-to-hours range.[151] While the thermal lifetimes are found to be strongly dependent on the nature of the solvent, also the different substitution pattern in DASAs (so the different generations) affect their thermal properties. The equilibrium between open and closed isomers in 1st generation DASAs is almost exclusively shifted towards the linear form in solution.[143,148,151] On the other hand, when accessing, the introduction of substituted aniline derivatives in 2nd generation DASAs stabilizes the closed form enough to allow a substantial amount of the cyclic form to be present at the thermodynamic equilibrium.[151] This feature was further addressed and improved with the introduction of the 3rd generation DASA photoswitches.[142] As in the spiropyran/merocyanine photochromic couple, the changes in chemical characteristics between the two photoisomers is very pronounced. Specifically, the open triene form is hydrophobic, while the closed form is hydrophilic and significantly more compact.[143,148] The open form can be stabilized even in polar solvents by adding a supramolecular complexing agent[145] (Scheme 18B), a strategy similar to the one discussed earlier for indirubin (*vide supra*), or by using metal-organic barrels in water.[152]

The photoisomerization behavior of DASAs is more complex compared to the other photochemical actuators we discussed and involves both photochemical and thermal steps.[153-157] A simplified picture is given in Figure 21. Excitation of the open form promotes the selective photochemical *Z*→*E* isomerization of the central C=C bond of the triene (**62**-A→**62**-A') (Scheme 19).[154,155] The presence of the hydroxy group favors the isomerization of this specific double bond, thanks to the introduction of steric interactions and by influencing its bond length.[157]

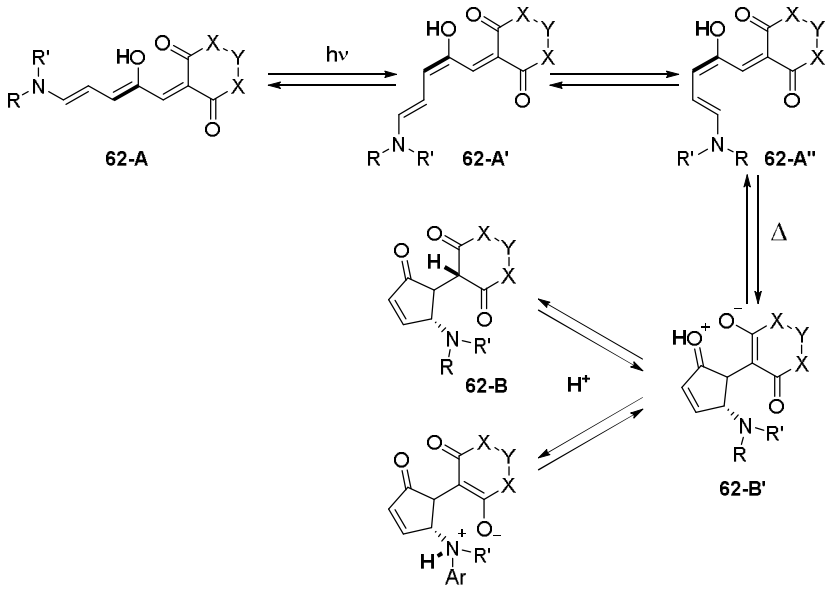

Scheme 19. Simplified (photo)isomerization mechanism of DASA photoswitches.

The C=C isomerization is ensued by a single-bond rotation of the neighboring C-C bond (**62**-A'→**62**-A"), a thermal ring-closure (**62**-A"→**62**-B'), and it is concluded by a H^+ transfer onto the donor or acceptor parts of the molecules, forming either of the compounds dubbed **62**-B in Scheme 19.[154,155]

The role of the hydroxy group connected to the central double bond crucial in the cyclization step. Non-hydroxy DASAs indeed only showed *E-Z* isomerization of the double bonds, without a marked selectivity, which did not lead to a productive cyclization step.[157] The nature of the solvent has notable effect on the overall switching process, however, the photochemical step is only affected at a limited extent, rendering the thermal **62**-A"→**62**-B' the rate determining step of the reaction.[156]

9. Conclusions

In summary, in this chapter we have discussed the characteristics of various classes of photochemical actuators based on an indole derivative. What is emerging from the studies presented in this review is the pivotal role that the introduction of heterocyclic derivatives based on indoles has on modifying the thermal and photochemical properties of the parent switches and motors. In this context, the sole introduction of the indole derivative is enough to grant novel steric and electronic properties that would have been obtained only by introducing more complex substitution patterns in the parent molecule. Indeed, only the introduction of the sole indole and oxindole motifs in a photochemical actuator often results in visible-light responsive compounds.

Novel pathways can be accessed, thanks to the *N*H function that represents the perfect handle for interactions with the environment. New pathways operating through proton transfer, both at the ground and excited state, can modulate the isomerization activity of the compound. On the other hand, the facile functionalization of the indolic nitrogen opens new avenues in terms of improvement of the absorption, photochemical and thermal properties.

Nonetheless, the rationalization and prediction of the isomerization pathways of the indole derivatives still remains a challenging task for the organic and physical organic chemists, in the task of synthesizing novel photochemical actuators. A concerted effort of the photochemical, theoretical and synthetic organic communities is necessary to let this sub-field strive, in order to advance the knowledge of molecular machinery driven by light stimuli.

Acknowledgements

We gratefully acknowledge the generous support from the Marie Skłodowska-Curie Actions (Individual Fellowship 838280 to SC) and the support by the Deutsche Forschungsgemeinschaft (DFG, German Research Foundation) under Germany's Excellence Strategy (EXC 2067/1- 390729940, NAS). We are indebted to Prof. Ben L. Feringa for his constant support in daring to try the unthinkable, Prof. Stefano Protti for his mentoring in the never-ending task to try to understand the complexity of the academic world and for his friendship.

References

1. Liu, S.; Zhao, F.; Chen, X.; Deng, G.; Huang, H. *Adv. Synth. Catal.* **2020**, *362*, 3795-3823.
2. Wen, J.; Shi, Z. *Acc. Chem. Res.* **2021**, *54*, 1723-1736.
3. Bandini, M.; Eichholzer, A. *Angew. Chem. Int. Ed.* **2009**, *48*, 9608-9644.
4. Dalpozzo, R. *Chem. Soc. Rev.* **2015**, *44*, 742-778.
5. de Sa Alves, F.; Barreiro, E.; Manssour Fraga, C. *Mini-Reviews Med. Chem.* **2009**, *9*, 782-793.
6. Evans, B. E.; Rittle, K. E.; Bock, M. G.; DiPardo, R. M.; Freidinger, R. M.; Whitter, W. L.; Lundell, G. F.; Veber, D. F.; Anderson, P. S.; Chang, R. S. L.; Lotti, V. J.; Cerino, D. J.; Chen, T. B.; Kling, P. J.; Kunkel, K. A.; Springer, J. P.; Hirshfield, J. *J. Med. Chem.* **1988**, *31*, 2235-2246.
7. Kumari, A.; Singh, R. K. *Bioorg. Chem.* **2019**, *89*, 103021.
8. Dhuguru, J.; Skouta, R. *Molecules* **2020**, *25*, 1615.
9. Dorababu, A. *RSC Med. Chem.* **2020**, *11*, 1335-1353.
10. Surur, A. S.; Huluka, S. A.; Mitku, M. L.; Asres, K. *Drug Des. Devel. Ther.* **2020**, *14*, 4855-4867.
11. Sharma, V.; Kumar, P.; Pathak, D. *J. Heterocycl. Chem.* **2010**, *47*, 491-502.
12. Yamazaki, S.; Sobolewski, A. L.; Domcke, W. *Phys. Chem. Chem. Phys.* **2011**, *13*, 1618-1628.
13. Kathan, M.; Hecht, S. *Chem. Soc. Rev.* **2017**, *46*, 5536-5550.
14. Albini, A.; Fagnoni, M. In *Green Chemical Reactions*; Tundo, P., Esposito, V., Eds.; Springer Netherlands: Dordrecht, 2008, 173-189.

15. Qian, X.; Yan, R.; Hang, Y.; Lv, Y.; Zheng, L.; Xu, C.; Hou, L. *Dyes Pigm.* **2017**, *139*, 274-282.
16. Barraja, P.; Sciabica, L.; Diana, P.; Lauria, A.; Montalbano, A.; Almerico, A. M.; Dattolo, G.; Cirrincione, G.; Disarò, S.; Basso, G.; Viola, G.; Dall'Acqua, F. *Bioorg. Med. Chem. Lett.* **2005**, *15*, 2291-2294.
17. Turro, N. J.; Ramamurthy, V.; Scaiano, J. C. *Modern Molecular Photochemistry of Organic Molecules*, 1st ed.; University Science Books: Sausalito, 2010.
18. Irie, M. *Pure Appl. Chem.* **2015**, *87*, 617-626.
19. Matsushima, R.; Sakaguchi, H. *J. Photochem. Photobiol. A Chem.* **1997**, *108*, 239-245.
20. Rybalkin, V. P.; Makarova, N. I.; Pluzhnikova, S. Y.; Popova, L. L.; Metelitsa, A. V.; Bren', V. A.; Minkina, V. I. *Russ. Chem. Bull.* **2014**, *63*, 1780-1784.
21. Kortekaas, L.; Browne, W. R. *Chem. Soc. Rev.* **2019**, *48*, 3406-3424.
22. Lerch, M. M.; Szymański, W.; Feringa, B. L. *Chem. Soc. Rev.* **2018**, *47*, 1910-1937.
23. Crespi, S.; Simeth, N. A.; König, B. *Nat. Rev. Chem.* **2019**, *3*, 133-146.
24. *Molecular Switches*; Feringa, B. L., Browne, W. R., Eds.; Wiley-VCH Verlag GmbH & Co. KGaA: Weinheim, Germany, 2011.
25. Koumura, N.; Zijlstra, R. W. J.; van Delden, R. A.; Harada, N.; Feringa, B. L. *Nature* **1999**, *401*, 152-155.
26. de Meijere, A. *Angew. Chem. Int. Ed.* **2005**, *44*, 7836-7840.
27. Baeyer, A.; Drewsen, V. *Ber. Dtsch. Chem. Ges.* **1882**, *15*, 2856-2864.
28. Steingruber, E. In *Ullmann's Encyclopedia of Industrial Chemistry*; Wiley-VCH Verlag GmbH & Co. KGaA: Weinheim, Germany, 2004.
29. Christie, R. M. *Colour Chemistry*; RSC Paperbacks; Royal Society of Chemistry: Cambridge, 2007.
30. Ross, D. L. *Appl. Opt.* **1971**, *10*, 571-576.
31. Memming, R.; Kobs, K. *Ber. Bunsenges. Phys. Chem.* **1981**, *85*, 238-242.
32. Koeppe, B.; Römpp, F. *Chem. Eur. J.* **2018**, *24*, 14382-14386.
33. Boice, G.; Patrick, B. O.; McDonald, R.; Bohne, C.; Hicks, R. *J. Org. Chem.* **2014**, *79*, 9196-9205.
34. Huang, C.-Y.; Bonasera, A.; Hristov, L.; Garmshausen, Y.; Schmidt, B. M.; Jacquemin, D.; Hecht, S. *J. Am. Chem. Soc.* **2017**, *139*, 15205-15211.
35. Farka, D.; Scharber, M.; Głowacki, E. D.; Sariciftci, N. S. *J. Phys. Chem. A* **2015**, *119*, 3563-3568.
36. Pina, J.; Sarmento, D.; Accoto, M.; Gentili, P. L.; Vaccaro, L.; Galvão, A.; Seixas de Melo, J. S. *J. Phys. Chem. B* **2017**, *121*, 2308-2318.
37. Christie, R. M. *Biotech. Histochem.* **2007**, *82*, 51-56.
38. Wyman, G. M. *Chem. Rev.* **1955**, *55*, 625-657.
39. Giuliano, C.; Hess, L.; Margerum, J. *J. Am. Chem. Soc.* **1968**, *90*, 587-594.
40. Weinstein, J.; Wyman, G. M. *J. Am. Chem. Soc.* **1956**, *78*, 4007-4010.
41. Koeppe, B.; Schröder, V. R. F. *ChemPhotoChem* **2019**, *3*, 613-619.
42. Tanaka, H.; Matsumoto, Y. *Heterocycles* **2003**, *60*, 1805-1810.
43. Huber, L. A.; Mayer, P.; Dube, H. *ChemPhotoChem* **2018**, *2*, 458-464.
44. Baeyer, A.; Emmerling, A. *Ber. Dtsch. Chem. Ges.* **1870**, *3*, 514-517.
45. Perpète, E. A.; Preat, J.; André, J.-M.; Jacquemin, D. *J. Phys. Chem. A* **2006**, *110*, 5629-5635.
46. Wyman, G. M. *J. Chem. Soc. D Chem. Commun.* **1971**, *21*, 1332-1334.
47. Thumser, S.; Köttner, L.; Hoffmann, N.; Mayer, P.; Dube, H. *J. Am. Chem. Soc.* **2021**, *143*, 18251-18260.
48. Kiss, F. L.; Corbet, B. P.; Simeth, N. A.; Feringa, B. L.; Crespi, S. *Photochem. Photobiol. Sci.* **2021**, *20*, 927-938.
49. Zhang, G.; Fu, Y.; Xie, Z.; Zhang, Q. *Macromolecules* **2011**, *44*, 1414-1420.
50. Luňák, S.; Horáková, P.; Lyčka, A. *Dyes Pigm.* **2010**, *85*, 171-176.
51. Huang, J.; Chen, Z.; Mao, Z.; Gao, D.; Wei, C.; Lin, Z.; Li, H.; Wang, L.; Zhang, W.; Yu, G. *Adv. Electron. Mater.* **2017**, *3*, 1700078.
52. Wee, X. K.; Yeo, W. K.; Zhang, B.; Tan, V. B. C.; Lim, K. M.; Tay, T. E.; Go, M.-L. *Bioorg. Med. Chem.* **2009**, *17*, 7562-7571.
53. Zhao, P.; Li, Y.; Gao, G.; Wang, S.; Yan, Y.; Zhan, X.; Liu, Z.; Mao, Z.; Chen, S.; Wang, L. *Eur. J.*

Med. Chem. **2014**, *86*, 165-174.
54. Wang, L.; Bai, S.; Wu, Y.; Liu, Y.; Yao, J.; Fu, H. *Angew. Chem. Int. Ed.* **2020**, *59*, 2003-2007.
55. Carrasco, M. P.; Machado, M.; Gonçalves, L.; Sharma, M.; Gut, J.; Lukens, A. K.; Wirth, D. F.; André, V.; Duarte, M. T.; Guedes, R. C.; dos Santos, D. J. V. A.; Rosenthal, P. J.; Mazitschek, R.; Prudêncio, M.; Moreira, R. *ChemMedChem* **2016**, *11*, 2194-2204.
56. Petermayer, C.; Dube, H. *Acc. Chem. Res.* **2018**, *51*, 1153-1163.
57. Petermayer, C.; Thumser, S.; Kink, F.; Mayer, P.; Dube, H. *J. Am. Chem. Soc.* **2017**, *139*, 15060-15067.
58. Zhao, X.; Yang, S. *J. Lumin.* **2020**, *220*, 116993.
59. Berdnikova, D. V. *Beilstein J. Org. Chem.* **2019**, *15*, 2822-2829.
60. Berdnikova, D. V. *Chem. Commun.* **2019**, *55*, 8402-8405.
61. Petermayer, C.; Dube, H. *J. Am. Chem. Soc.* **2018**, *140*, 13558-13561.
62. Wiedbrauk, S.; Dube, H. *Tetrahedron Lett.* **2015**, *56*, 4266-4274.
63. Sailer, A.; Ermer, F.; Kraus, Y.; Lutter, F. H.; Donau, C.; Bremerich, M.; Ahlfeld, J.; Thorn-Seshold, O. *ChemBioChem* **2019**, *20*, 1305-1314.
64 Cordes, T.; Weinrich, D.; Kempa, S.; Riesselmann, K.; Herre, S.; Hoppmann, C.; Rück-Braun, K.; Zinth, W. *Chem. Phys. Lett.* **2006**, *428*, 167-173.
65. Huber, L. A.; Hoffmann, K.; Thumser, S.; Böcher, N.; Mayer, P.; Dube, H. *Angew. Chem. Int. Ed.* **2017**, *56*, 14536-14539.
66. Gerwien, A.; Mayer, P.; Dube, H. *Nat. Commun.* **2019**, *10*, 4449.
67. Guentner, M.; Schildhauer, M.; Thumser, S.; Mayer, P.; Stephenson, D.; Mayer, P. J.; Dube, H. *Nat. Commun.* **2015**, *6*, 8406.
68. Wilcken, R.; Schildhauer, M.; Rott, F.; Huber, L. A.; Guentner, M.; Thumser, S.; Hoffmann, K.; Oesterling, S.; de Vivie-Riedle, R.; Riedle, E.; Dube, H. *J. Am. Chem. Soc.* **2018**, *140*, 5311-5318.
69. Uhl, E.; Thumser, S.; Mayer, P.; Dube, H. *Angew. Chem. Int. Ed.* **2018**, *57*, 11064-11068.
70 Hoorens, M. W. H.; Medved', M.; Laurent, A. D.; Di Donato, M.; Fanetti, S.; Slappendel, L.; Hilbers, M.; Feringa, B. L.; Jan Buma, W.; Szymanski, W. *Nat. Commun.* **2019**, *10*, 2390.
71. Medved', M.; Hoorens, M. W. H.; Di Donato, M.; Laurent, A. D.; Fan, J.; Taddei, M.; Hilbers, M.; Feringa, B. L.; Buma, W. J.; Szymanski, W. *Chem. Sci.* **2021**, *12*, 4588-4598.
72. Crespi, S.; Simeth, N. A.; Di Donato, M.; Doria, S.; Stindt, C. N.; Hilbers, M. F.; Kiss, F. L.; Toyoda, R.; Wesseling, S.; Buma, W. J.; Feringa, B. L.; Szymanski, W. *Angew. Chem. Int. Ed.* **2021**, *60*, 25290-25295.
73. Feringa, B. L. *Angew. Chem. Int. Ed.* **2017**, *56*, 11060-11078.
74. Kathan, M.; Hecht, S. *Chem. Soc. Rev.* **2017**, *46*, 5536-5550.
75. Costil, R.; Holzheimer, M.; Crespi, S.; Simeth, N. A.; Feringa, B. L. *Chem. Rev.* **2021**, *121*, 13213-13237.
76. Zhang, Q.; Qu, D.-H.; Tian, H.; Feringa, B. L. *Matter* **2020**, *3*, 355-370.
77. Krause, S.; Feringa, B. L. *Nat. Rev. Chem.* **2020**, *4*, 550-562.
78. Dorel, R.; Feringa, B. L. *Angew. Chem. Int. Ed.* **2020**, *59*, 785-789.
79. Chen, K.-Y.; Ivashenko, O.; Carroll, G. T.; Robertus, J.; Kistemaker, J. C. M.; London, G.; Browne, W. R.; Rudolf, P.; Feringa, B. L. *J. Am. Chem. Soc.* **2014**, *136*, 3219-3224.
80. Pooler, D. R. S.; Lubbe, A. S.; Crespi, S.; Feringa, B. L. *Chem. Sci.* **2021**, *12*, 14964-14986.
81. Kistemaker, J. C. M.; Štacko, P.; Roke, D.; Wolters, A. T.; Heideman, G. H.; Chang, M.-C.; van der Meulen, P.; Visser, J.; Otten, E.; Feringa, B. L. *J. Am. Chem. Soc.* **2017**, *139*, 9650-9661.
82. Roke, D.; Wezenberg, S. J.; Feringa, B. L. *Proc. Natl. Acad. Sci.* **2018**, *115*, 9423-9431.
83. Roke, D.; Sen, M.; Danowski, W.; Wezenberg, S. J.; Feringa, B. L. *J. Am. Chem. Soc.* **2019**, *141*, 7622-7627.
84. Pooler, D. R. S.; Pierron, R.; Crespi, S.; Costil, R.; Pfeifer, L.; Léonard, J.; Olivucci, M.; Feringa, B. L. *Chem. Sci.* **2021**, *12*, 7486-7497.
85. Paolino, M.; Giovannini, T.; Manathunga, M.; Latterini, L.; Zampini, G.; Pierron, R.; Léonard, J.; Fusi, S.; Giorgi, G.; Giuliani, G.; Cappelli, A.; Cappelli, C.; Olivucci, M. *J. Phys. Chem. Lett.* **2021**, *12*, 3875-3884.

86. Hartley, G. S. *Nature* **1937**, *140*, 281.
87. Simeth, N. A.; Crespi, S. In *Photochemistry: Volume 48*; The Royal Society of Chemistry, 2021; Vol. 48, 344-375.
88. Crespi, S.; Simeth, N. A.; Bellisario, A.; Fagnoni, M.; König, B. *J. Phys. Chem. A* **2019**, *123*, 1814-1823.
89. Simeth, N. A.; Crespi, S.; Fagnoni, M.; König, B. *J. Am. Chem. Soc.* **2018**, *140*, 2940-2946.
90. Xu, Y.; Gao, C.; Andréasson, J.; Grøtli, M. *Org. Lett.* **2018**, *20*, 4875-4879.
91. Jacob, N.; Guillemard, L.; Wencel-Delord, J. *Synthesis* **2020**, *52*, 574-580.
92. Simeth, N. A.; Bellisario, A.; Crespi, S.; Fagnoni, M.; König, B. *J. Org. Chem.* **2019**, *84*, 6565-6575.
93. Calbo, J.; Weston, C. E.; White, A. J. P.; Rzepa, H. S.; Contreras-García, J.; Fuchter, M. J. *J. Am. Chem. Soc.* **2017**, *139*, 1261-1274.
94. Crespi, S.; Simeth, N. A.; Bellisario, A.; Fagnoni, M.; König, B. *J. Phys. Chem. A* **2019**, *123*, 1814-1823.
95. Irie, M. *Chem. Rev.* **2000**, *100*, 1685-1716.
96. Irie, M.; Fukaminato, T.; Matsuda, K.; Kobatake, S. *Chem. Rev.* **2014**, *114*, 12174-12277.
97. Cheng, H.-B.; Tan, X.; Pang, M.-L. *Eur. J. Org. Chem.* **2013**, *2013*, 7933-7940.
98. Nakamura, S.; Yokojima, S.; Uchida, K.; Tsujioka, T.; Goldberg, A.; Murakami, A.; Shinoda, K.; Mikami, M.; Kobayashi, T.; Kobatake, S.; Matsuda, K.; Irie, M. *J. Photochem. Photobiol. A Chem.* **2008**, *200*, 10-18.
99. Vomasta, D. University of Regensburg, 2009.
100. Fleming, C.; Remón, P.; Li, S.; Simeth, N. A.; König, B.; Grøtli, M.; Andréasson, J. *Dyes Pigm.* **2017**, *137*, 410-420.
101. Irie, M.; Sayo, K. *J. Phys. Chem.* **1992**, *96*, 7671-7674.
102. Zheng, C.; Liao, G.; Fan, C.; Wang, R.; Pu, S. *J. Chem. Res.* **2017**, *41*, 423-426.
103. Saita, S.; Yamaguchi, T.; Kawai, T.; Irie, M. *ChemPhysChem* **2005**, *6*, 2300-2306.
104. Du, H.; Gao, S.; Yang, L. *Int. J. Org. Chem.* **2012**, *02*, 387-390.
105. Giordano, L.; Vermeij, R. J.; Jares-Erijman, E. A. *Arkivoc* **2006**, *2005*, 268-281.
106. Sun, Z.; Li, H.; Liu, G.; Fan, C.; Pu, S. *Dyes Pigm.* **2014**, *106*, 94-104.
107. Singer, M.; Nierth, A.; Jäschke, A. *Eur. J. Org. Chem.* **2013**, *2013*, 2766-2769.
108. Huang, Z.-N.; Jin, S.; Ming, Y.; Fan, M. *Mol. Cryst. Liq. Cryst. Sci. Technol. Sect. A. Mol. Cryst. Liq. Cryst.* **1997**, *297*, 99-106.
109. Yokoyama, Y. *Chem. Rev.* **2000**, *100*, 1717-1740.
110. Wutz, D.; Gluhacevic, D.; Chakrabarti, A.; Schmidtkunz, K.; Robaa, D.; Erdmann, F.; Romier, C.; Sippl, W.; Jung, M.; König, B. *Org. Biomol. Chem.* **2017**, *15*, 4882-4896.
111. Renth, F.; Siewertsen, R.; Temps, F. *Int. Rev. Phys. Chem.* **2013**, *32*, 1-38.
112. Simeth, N. A.; Altmann, L.-M.; Wössner, N.; Bauer, E.; Jung, M.; König, B. *J. Org. Chem.* **2018**, *83*, 7919-7927.
113. Chen, X.; Islamova, N. I.; Robles, R. V.; Lees, W. J. *Photochem. Photobiol. Sci.* **2011**, *10*, 1023-1029.
114. Slavov, C.; Boumrifak, C.; Hammer, C. A.; Trojanowski, P.; Chen, X.; Lees, W. J.; Wachtveitl, J.; Braun, M. *Phys. Chem. Chem. Phys.* **2016**, *18*, 10289-10296.
115. Liang, Y.; Dvornikov, A. S.; Rentzepis, P. M. *Macromolecules* **2002**, *35*, 9377-9382.
116. Chen, X.; Islamova, N. I.; Garcia, S. P.; Di Girolamo, J. A.; Lees, W. J. *J. Org. Chem.* **2009**, *74*, 6777-6783.
117. Andréasson, J.; Straight, S. D.; Moore, T. A.; Moore, A. L.; Gust, D. *J. Am. Chem. Soc.* **2008**, *130*, 11122-11128.
118. Weerasekara, R. K.; Uekusa, H.; Hettiarachchi, C. V. *Cryst. Growth Des.* **2017**, *17*, 3040-3047.
119. Rustler, K.; Maleeva, G.; Gomila, A. M. J.; Gorostiza, P.; Bregestovski, P.; König, B. *Chem. Eur. J.* **2020**, *26*, 12722-12727.
120. Kohno, Y.; Tamura, Y.; Matsushima, R. *J. Photochem. Photobiol. A Chem.* **2009**, *201*, 98-101.
121. Seibold, M.; Handschuh, M.; Port, H.; Wolf, H. C. *J. Lumin.* **1997**, *72-74*, 454-456.
122. Volarić, J.; Szymanski, W.; Simeth, N. A.; Feringa, B. L. *Chem. Soc. Rev.* **2021**, *50*, 12377-12449.
123. Vlajić, M.; Unger, W.; Bruns, J.; Rueck-Braun, K. *Appl. Surf. Sci.* **2019**, *465*, 686-692.

124. Lachmann, D.; Konieczny, A.; Keller, M.; König, B. *Org. Biomol. Chem.* **2019**, *17*, 2467-2478.
125. Lachmann, D.; Lahmy, R.; König, B. *Eur. J. Org. Chem.* **2019**, *2019*, 5018-5024.
126. Straight, S. D.; Terazono, Y.; Kodis, G.; Moore, T. A.; Moore, A. L.; Gust, D. *Aust. J. Chem.* **2006**, *59*, 170-174.
127. Kurosaki, Y.; Sagisaka, T.; Matsushima, T.; Ubukata, T.; Yokoyama, Y. *ChemPhysChem* **2020**, *21*, 1375-1383.
128. Andréasson, J.; Straight, S. D.; Moore, T. A.; Moore, A. L.; Gust, D. *J. Am. Chem. Soc.* **2008**, *130*, 11122-11128.
129. Andrews, M. C.; Peng, P.; Rajput, A.; Cozzolino, A. F. *Photochem. Photobiol. Sci.* **2018**, *17*, 432-441.
130. Avagliano, D.; Sánchez-Murcia, P. A.; González, L. *Phys. Chem. Chem. Phys.* **2019**, *21*, 8614-8618.
131. Fleming, C. L.; Li, S.; Grøtli, M.; Andréasson, J. *J. Am. Chem. Soc.* **2018**, *140*, 14069-14072.
132. Kortekaas, L.; Chen, J.; Jacquemin, D.; Browne, W. R. *J. Phys. Chem. B* **2018**, *122*, 6423-6430.
133. Klajn, R. *Chem. Soc. Rev.* **2014**, *43*, 148-184.
134. Hammarson, M.; Nilsson, J. R.; Li, S.; Beke-Somfai, T.; Andréasson, J. *J. Phys. Chem. B* **2013**, *117*, 13561-13571.
135. Görner, H. *Phys. Chem. Chem. Phys.* **2001**, *3*, 416-423.
136. Brieke, C.; Heckel, A. *Chem. Eur. J.* **2013**, *19*, 15726-15734.
137. Steen, J. D.; Duijnstee, D. R.; Sardjan, A. S.; Martinelli, J.; Kortekaas, L.; Jacquemin, D.; Browne, W. R. *J. Phys. Chem. A* **2021**, *125*, 3355-3361.
138. Murase, N.; Ando, T.; Ajiro, H. *J. Mater. Chem. B* **2020**, *8*, 1489-1495.
139. Opel, J.; Rosenbaum, L.-C.; Brunner, J.; Staiger, A.; Zimmermanns, R.; Kellermeier, M.; Gaich, T.; Cölfen, H.; García-Ruiz, J.-M. *J. Mater. Chem. B* **2020**, *8*, 4831-4835.
140. Berton, C.; Busiello, D. M.; Zamuner, S.; Solari, E.; Scopelliti, R.; Fadaei-Tirani, F.; Severin, K.; Pezzato, C. *Chem. Sci.* **2020**, *11*, 8457-8468.
141. Hemmer, J. R.; Poelma, S. O.; Treat, N.; Page, Z. A.; Dolinski, N. D.; Diaz, Y. J.; Tomlinson, W.; Clark, K. D.; Hooper, J. P.; Hawker, C.; Read de Alaniz, J. *J. Am. Chem. Soc.* **2016**, *138*, 13960-13966.
142. Hemmer, J. R.; Page, Z. A.; Clark, K. D.; Stricker, F.; Dolinski, N. D.; Hawker, C. J.; Read de Alaniz, J. *J. Am. Chem. Soc.* **2018**, *140*, 10425-10429.
143. Helmy, S.; Leibfarth, F. A.; Oh, S.; Poelma, J. E.; Hawker, C. J.; Read de Alaniz, J. *J. Am. Chem. Soc.* **2014**, *136*, 8169-8172.
144. Sanchez, D. M.; Raucci, U.; Ferreras, K. N.; Martínez, T. J. *J. Phys. Chem. Lett.* **2020**, *11*, 7901-7907.
145. Mallo, N.; Tron, A.; Andréasson, J.; Harper, J. B.; Jacob, L. S. D.; McClenaghan, N. D.; Jonusauskas, G.; Beves, J. E. *ChemPhotoChem* **2020**, *4*, 407-412.
146. Duan, Y.; Zhao, H.; Xiong, C.; Mao, L.; Wang, D.; Zheng, Y. *Chinese J. Chem.* **2021**, *39*, 985-998.
147. Sroda, M. M.; Stricker, F.; Peterson, J. A.; Bernal, A.; Read de Alaniz, J. *Chem. Eur. J.* **2021**, *27*, 4183-4190.
148. Helmy, S.; Oh, S.; Leibfarth, F. A.; Hawker, C. J.; Read de Alaniz, J. *J. Org. Chem.* **2014**, *79*, 11316-11329.
149. Mallo, N.; Foley, E. D.; Iranmanesh, H.; Kennedy, A. D. W.; Luis, E. T.; Ho, J.; Harper, J. B.; Beves, J. E. *Chem. Sci.* **2018**, *9*, 8242-8252.
150. Aiken, S.; Edgar, R. J. L.; Gabbutt, C. D.; Heron, B. M.; Hobson, P. A. *Dyes Pigm.* **2018**, *149*, 92-121.
151. Mallo, N.; Brown, P. T.; Iranmanesh, H.; MacDonald, T. S. C.; Teusner, M. J.; Harper, J. B.; Ball, G. E.; Beves, J. E. *Chem. Commun.* **2016**, *52*, 13576-13579.
152. Saha, R.; Devaraj, A.; Bhattacharyya, S.; Das, S.; Zangrando, E.; Mukherjee, P. S. *J. Am. Chem. Soc.* **2019**, *141*, 8638-8645.
153. Zulfikri, H.; Koenis, M. A. J.; Lerch, M. M.; Di Donato, M.; Szymański, W.; Filippi, C.; Feringa, B. L.; Buma, W. J. *J. Am. Chem. Soc.* **2019**, *141*, 7376-7384.
154. Di Donato, M.; Lerch, M. M.; Lapini, A.; Laurent, A. D.; Iagatti, A.; Bussotti, L.; Ihrig, S. P.; Medved', M.; Jacquemin, D.; Szymański, W.; Buma, W. J.; Foggi, P.; Feringa, B. L. *J. Am. Chem. Soc.* **2017**, *139*, 15596-15599.
155. Lerch, M. M.; Wezenberg, S. J.; Szymanski, W.; Feringa, B. L. *J. Am. Chem. Soc.* **2016**, *138*, 6344-

6347.
156. Lerch, M. M.; Di Donato, M.; Laurent, A. D.; Medved', M.; Iagatti, A.; Bussotti, L.; Lapini, A.; Buma, W. J.; Foggi, P.; Szymański, W.; Feringa, B. L. *Angew. Chem. Int. Ed.* **2018**, *57*, 8063-8068.
157. Lerch, M. M.; Medved′, M.; Lapini, A.; Laurent, A. D.; Iagatti, A.; Bussotti, L.; Szymański, W.; Buma, W. J.; Foggi, P.; Di Donato, M.; Feringa, B. L. *J. Phys. Chem. A* **2018**, *122*, 955-964.